ISET Journal of Earthquake Technology, Paper No. 530, Vol. 52, No. 1, March 2015, pp. 1–28

RE-QUALIFICATION OF NON-SEISMICALLY DESIGNED EXISTING STRUCTURES THROUGH TUNED SLOSHING WATER DAMPERS: AN EXPERIMENTAL STUDY

Nishant Kishore Rai*, G.R. Reddy** and V. Venkatraj*
*DCSEM, DAE, Mumbai, India
**BARC, DAE, Mumbai, India

ABSTRACT

Existing medium height RC frame structures with masonry infill panels can be made earthquake safe by limiting the story drift to 0.2% and thereby ensuring compressive strut action of masonry panels in load resisting mechanism. The tuned sloshing water damper (TSWD) is an effective system for reducing displacement response of structures. The TSWD based systems are sensitive to characteristics of host structures and excitations imposed. The single frequency TSWD systems can be optimally designed and executed for targeted response control of accurately assessed structures against well-defined excitations. The multiple frequency TSWD is a robust system for response control of approximately assessed structures against dynamic excitations. A simulated shake table experimental study has been conducted on a reduced scale model of an existing structure. A retrofitting regime for 25% displacement response reduction of the existing structure has been proposed with multiple frequency TSWD system mounted on its roof. The reduced response shall limit the story drift and ensure the compressive strut action of masonry panels.

KEYWORDS: Story Drift, Effective Damping Ratio, Mass Ratio, Effectiveness Ratio and Specific Mass Ratio

INTRODUCTION

The Existing RC framed buildings constructed without special seismic detailing may resist minor to moderate earthquakes, but their performance under severe earthquakes may be extremely poor (Bracci et al. 1997). The disastrous consequences of such structures exposed to a strong seismic eventuality have been demonstrated through 25.04.15, Lamjung, Nepal, earthquake.

These existing RC framed structures are provided with masonry infill panel. The re-qualification of such existing structures against earthquake has been explored by considering interaction of infill masonry panels with surrounding RC frames. The structural contribution of masonry panel can be accounted as diagonal compressive strut (Holmes, 1961). The structural contribution of masonry infill enhances overall performance of the structures against lateral loads at small story drifts but at large story drifts the performance enhancement disappears (Mehrabi et al., 1996). The restricted story drift of existing structures shall ensure diagonal strut action of masonry panel along with RC frame leading to safety against earthquake. This paper proposes to restrict the story drift by tuned sloshing water damper (TSWD) based response control system.

A TSWD, used for structural response control, consists of water tank, rigidly attached with the host structure (Figure 1). The response control characteristics of the TSWDs are like that of tuned mass damper (TMD) with sloshing water as damper mass. The characteristics of TSWDs such as frequency (ω_d) and damping ratio (ξ_d) are dependent on amplitude of excitation (A_e) of TSWD and are determined empirically (Yu, 1999; Yalla, 2001; Tait, 2008). The effectiveness of TSWD based retrofitting system is sensitive to its tuning with respect to frequency (ω_s) and damping ratio (ξ_s) of the host structure. The TSWD based retrofitting system may be designed and constructed in tuning with the principal axes of the host structure offering functionality in all possible directions in horizontal plane (Rai et al., 2011).

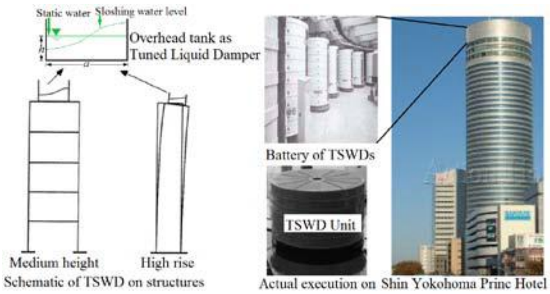

Fig. 1 TSWD on a structure

For seismic retrofitting of existing structures, the optimal tuning of a single frequency TSWD (STSWD) system is difficult to achieve. Multi-frequency tuned sloshing water dampers (MTSWD) in place of STSWD have been used for seismic response control of multi-modal structures. The damping mass is distributed among more than one prominent modal frequencies of the host structure. The MTSWD system is conveniently applicable to real life structures by accommodating required sloshing mass in multiple tanks. These tanks can be tuned with respect to several modal frequencies of the structure forming a MTSWD system. With the same damping mass, as in STSWD, MTSWDs are more effective to reduce responses of multi-modal high-rise structures subjected to broad band excitations (Koh et al., 1995; Li and Wang, 2004).

This paper explores the effectiveness of STSWD system and MTSWD system on approximately assessed existing structure subjected to dynamic excitations. Shake table simulated experiments have been conducted on reduced scaled model (SM) of an existing structure (ES) in coupling with STSWD and MTSWD systems. The performances of both systems have been evaluated and a retrofitting scheme for ES has been proposed.

STATE OF EXISTING STRUCTURES AND RETROFITTING STRATEGY

The RC frames constructed without special seismic detailing are termed as non-ductile RC frame. The non-ductile RC framed structures with infill masonry panels forms a major chunk of the existing building stock around the world. The infill masonry is constructed after casting the RC frames and slabs. These structures have been designed for gravity loads only. The Earthquake Engineering Research Institute and International Association for Earthquake Engineering have conducted comprehensive survey of existing buildings in earthquake prone areas (Jaiswal et al., 2002; Heidi et al., 2004; Marhatta et al., 2007). The existing non-ductile moment resisting framed buildings are seismically vulnerable across the world and must be retrofitted earnestly.

1. Interaction of Infill Masonry Panels with RC Frame

The lateral load resisting capacity provided by non-ductile RC frames are nominal. The structural contribution of infill masonry can significantly increase the lateral strength of RC frames. The interactions between infill masonry panels with RC frame is an area of intense research for seismic requalification of existing structures. The significant observations of these studies are mentioned below:

a) The interaction between the infill masonry wall and the surrounding frame enhances overall stiffness and in-plane moment of inertia of the RC and masonry composite frame. The shock tests on the masonry in-filled RC frames exhibits, that at low excitation levels at base, acceleration gets amplified at roof, exhibiting an almost elastic behaviour. (Dolšek and Fajfar, 2008; Kose, 2009; Rodrigues et al., 2010).
b) The masonry infill increases the building strength by 50%; however, this additional strength disappears at comparatively small lateral drifts (Valiasis and Stylianidis, 1989).
c) The overall behaviour of composite frame is dependent on RC frame material, strength of masonry units and its mortar. The crack of infill has been reported at small lateral drift (<0.2%). The masonry panels reach their ultimate strength at 0.3% drift (Manos et al., 1995; Pires et al., 1995).
d) The structural contribution of masonry panels may be accounted as diagonal compressive struts of effective width w_d. Panels with openings for doors/ windows are represented by diagonal struts of

reduced effective width w_{do} (Figure 2). The structural contribution of panels having more than 40% opening is negligible (Mondal, 2003).

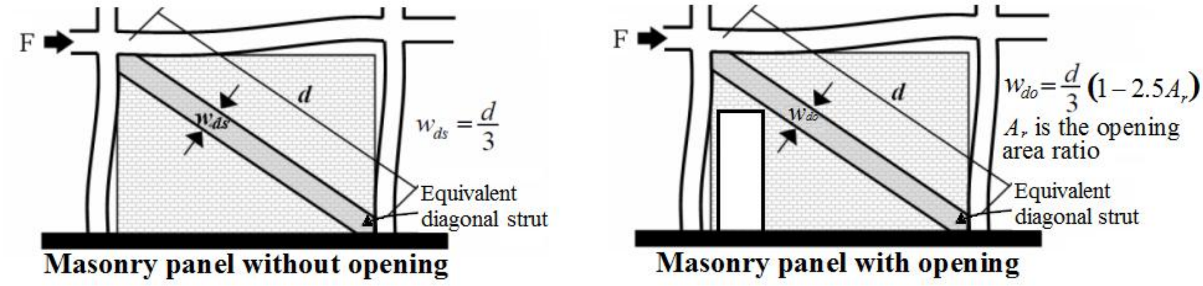

Fig. 2 Equivalent diagonal struts

It may be inferred that during a seismic eventuality if the failure of masonry panels is avoided, then the RC-masonry composite frame structures remain linearly elastic.

2. Damping Ratio of Existing Structures

The response of structures against dynamic loads depend on inherent damping ratio. A typical 5% damping ratio is implicit in the code specified earthquake forces and design spectrums (Chopra, 1995). The response correction factors are suggested for damping ratios other than 5%, indicating decreasing response with increase of damping ratio (Nawrotzki, 2005). The structures, designed with working stress method, exhibiting no visible cracks in structural elements and separation crack at interface between RC fame and masonry may possess damping ratio of 3% (Newmark and Hall, 1978).

3. Existing Structure for Present Study

For the present study, the structures of a township in Mumbai, India has been considered as representative of existing building stock of urban India. The structures are adequately designed and constructed in accordance with the prevalent code (BIS: 456-2000). These structures are in seismic zone III of BIS:1893 classification. The structures have been analysed for gravity and seismic loads. The seismic analysis with 5% damping ratio has been done for two structural conditions:

a) Bare frame: only RC members are acting in load resisting mechanism.
b) RC-Masonry composite frame: 230 mm thick infill masonry is contributing as compressive diagonal strut along with RC members in load resisting mechanism.

The descriptive data for these buildings are tabulated in Table 1.

Table 1: Details of Masonry Infilled RC Framed Buildings

Type of Building and Area of Accommodation	Number of Storey	Total Load (kN)	% Contribution in Loading				
			Live Load	RC frame	RC Slab	Finishes	Masonry
Residential: 3 BHK units of 95sqm. each, 2 units per floor	3	8950	10.2	30.2	15.9	7.9	35.8
	4	11640	10.7	28.9	16.2	8.0	36.2
	7	19120	11.7	30.0	17.1	8.3	32.9
	8	22040	11.7	30.1	16.9	8.2	33.1
Residential: 2 BHK units of 54sqm. each, 2 units per floor	3	5510	9.8	31.5	14.3	8.1	36.3
	5	8790	10.5	30.9	14.4	8.0	36.2
School, 1920 sqm	4	31030	16.7	26.6	21.0	9.2	26.5
Institutional/office 920sq.m	4	12770	17.7	25.9	24.9	9.8	21.7

The maximum column stresses obtained from seismic analysis have been normalised with respect to maximum column stress under gravity load for which structure has been designed and constructed. The maximum normalised column stresses for each type of building are presented in Table 2.

Table 2: Normalised Maximum Column Stress Due to Seismic Loads

Type of Building	Number of Storey	Normalised Maximum Stress			Number of Columns Governed by Seismic Loading
		Gravity	Earthquake		
			Bare Frame	RC-Masonry Composite Frame	
3 BHK units of 95sqm. each, 2 units per floor	3	1	1.53	1.04	6 out of 30
	4	1	1.74	1.11	26 out of 30
	7	1	1.34	1.06	22 out of 30
	8	1	1.30	1.04	24 out of 30
2 BHK units of 54sqm. each, 2 units per floor	3	1	1.18	0.86	16 out of 24
	5	1	1.26	0.91	20 out of 24
School	4	1	1.38	0.97	28 out of 32
Institutional/office	4	1	1.37	1.03	18 out of 20

It is evident from Table 2 that for bare frame condition all the structures have exceeded the maximum column stresses under earthquake loading. However, with structural contribution of masonry the stress levels are brought within safety limits. The existing structures may be made safe against earthquake by ensuring structural contribution from masonry as compressive diagonal strut. The 4-story residential building, being worst stressed during seismic eventuality, has been chosen for detailed retrofitting studies.

4. Details of the Four-Story Residential Building

The existing four story residential building (ES) houses 8 flats with a centrally located staircase, over which overhead tank (OHT) is placed. The ES is founded on firm strata at 2.5 m depth from plinth level. The existing building and its structural skeleton is shown in Figure 3.

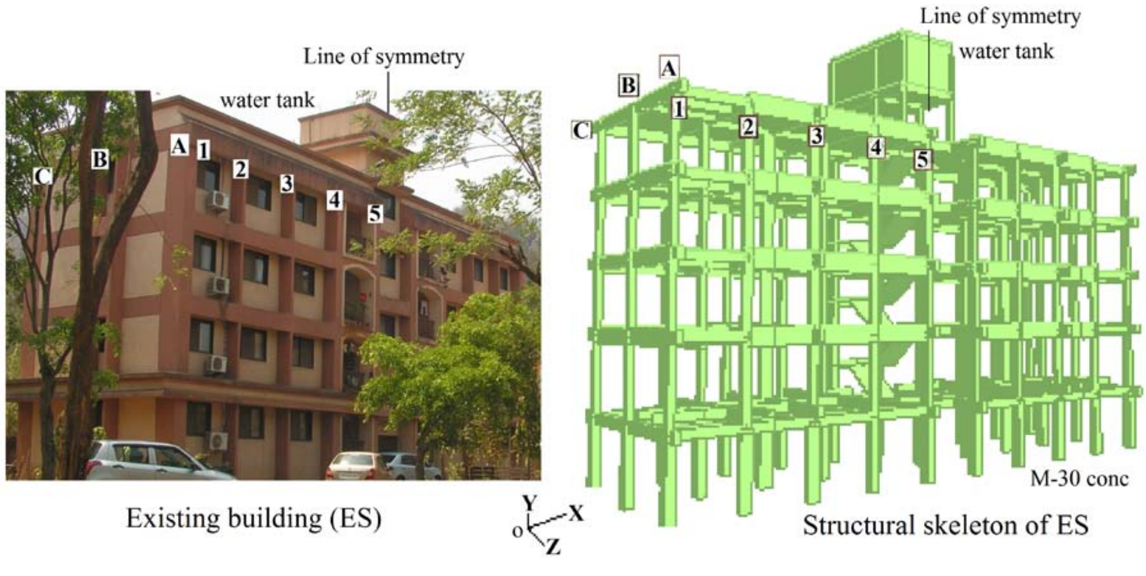

Fig. 3 Existing building (ES) and its structural skeleton (RC frame)

The RC frame has been constructed in M-30 grade of concrete with Fe-415 grade of reinforcement. The burnt clay brick masonry has been built after RC frame construction. External walls are 230 mm thick in 1:6 cement-sand mortar and internal partition walls are 115 mm thick in 1:4 cement-sand mortar. A skin plaster of 1:6 cement-sand mortar, continuous over RC members and masonry, has been provided. The typical floor plan with column, beam and masonry layout is shown in Figure 4.

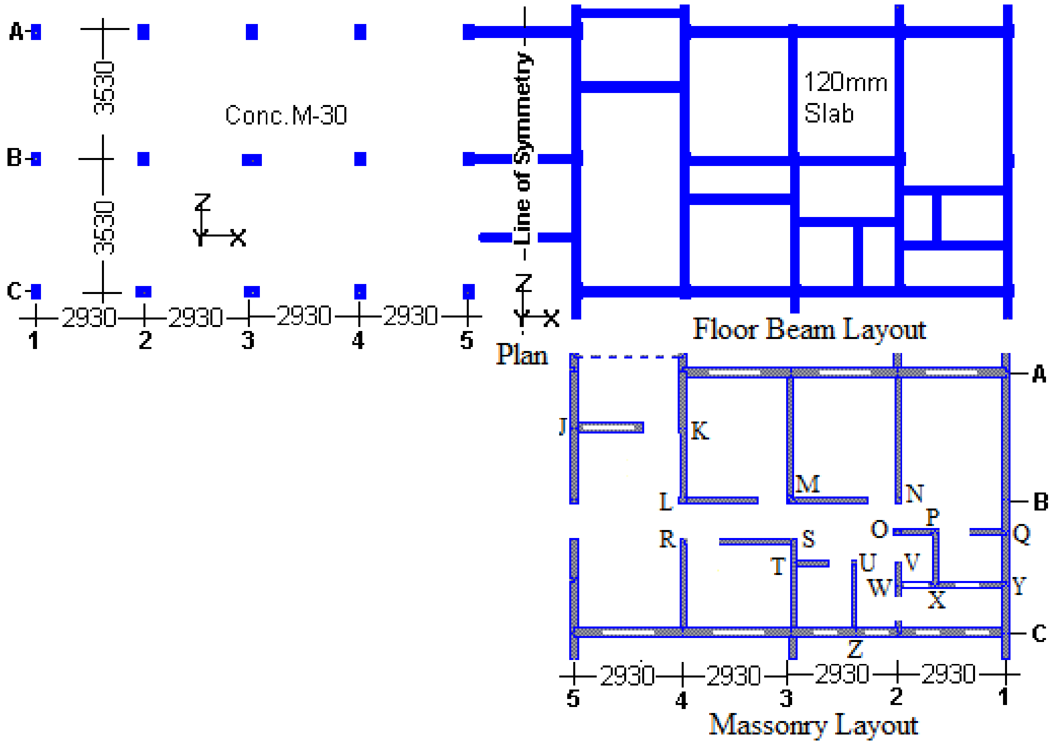

Fig. 4 Structural floor plan and masonry layout of existing structure 'ES'

The details of RC members of the structure have been given in Table 3.

Table 3: Details of RC Members

Structural Member	Size (mm)	Level	Length(m)
Columns C1 to C5, B1, B2, B4, B5 and A1 to A5	350 x 450	Below plinth	2.5
Column B3	350 x 600	Below plinth	2.5
Columns C1 to C5, B1, B2, B4, B5 and A1 to A5	250 x 350	Plinth level to roof	2.95
Columns A5, B5 and C5	250 x 250	Roof to OHT base.	2.4
Column B3	250 x 500	Plinth level to roof	2.95
Beams along X between A1 to A5, B1 to B5 and C1 to C5	250 x 400	At plinth and all floor levels	2.93
Beams along Z between A1 to C1, A2 to C2, A3 to C3, A4 to C4 and A5 to C5	250 x 450	At plinth and all floor levels	3.53
Suspended slab at plinth level	100	At plinth (+450) mm level	
Floor slabs and landings of staircase	120		
Stair case waist slab	140		
Overhead water tank base slab	200		
Overhead water tank walls	150		

The details of masonry panels and corresponding equivalent compressive diagonal struts are given in Table 4.

Table 4: Details of Masonry Panel

Panel Id	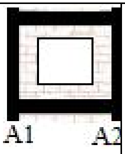	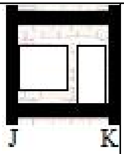	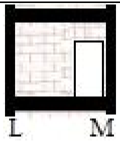	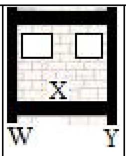	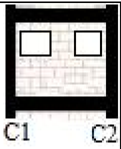	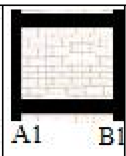	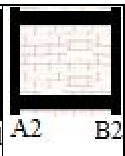	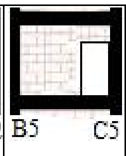	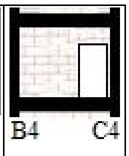
Panel Location	Along X between A1 to A4	Along X between J-K	Along X between L-M; M-N; R-S and O-P-Q	Along X between W-Y	Along X between C1 to C2	Along Z between A1-B1; B1-C1 and A5-B5	Along Z between A2-B2; A3-B3 and A4-B4	Along Z between B5-C5	Along Z between B3-C3 and B4-C4
Dimen-sions (m)	2.55 x 2.68 x 0.23	2.55 x 2.68 x 0.23	2.55x 2.68 x 0.115	2.55x 2.68 x 0.115	2.55 x 2.68 x0.23	2.50 x 3.24 x 0.23	2.50 x 3.24 x 0.115	2.50 x 3.24 x0.23	2.50x 3.24 x 0.115
Strength (MPa)	0.44	0.44	0.5	0.5	0.44	0.44	0.5	0.44	0.5
Opening	1.2 x 1.2	1.2 x 1.2 and 0.9 x 2.1	0.9 x 2.1	2 openings 0.6x 0.6	2 openings 0.6x 0.6	no opening	no opening	0.9 x 2.1	0.9 x 2.1
Effective Depth (mm)	746	Ignored	381	908	908	1364	1364	568	568

5. Analytical Scrutiny of Structural Performance

The structure has been analytically modelled and scrutinised for seismic conditions of zone-III as per IS1893 (Part-1) provisions. The scrutiny has been discretised in six combinations of loads and structural conditions as given in Table 5.

Table 5: Discretisation of ES

Case Id	**Loads Imposed**	**Load Resisting Mechanism**	**Damping Ratio**
Case1	1.2 times static gravity	Bare RC frame	Not applicable
Case2	Seismic + Gravity	Bare RC frame	5%
Case3	Seismic + Gravity	RC-Masonry composite (all masonry panels are contributing)	5%
Case4	Seismic + Gravity	RC-Masonry composite (Only 230 mm masonry is contributing)	5%
Case5	Seismic + Gravity	RC-Masonry composite (all masonry panels are contributing)	3%
Case6	Seismic + Gravity	RC-Masonry composite (Only 230 mm masonry is contributing)	3%

The salient features of the ES obtained from analysis are given in Table 6.

Table 6: Salient Features of Existing Structure

Feature and Condition		Value
Total weight of structure		1164000 kg (water tank full)
Mass participation in first mode m_s		76% (885000 kg).
Structural damping ratio ξ_s	Bare RC frame	5% (code provision)
	With masonry infill	3%
First mode frequency of ES 'ω_s' (masonry infill)	Case 3 and Case 5	1.803 Hz along X; 1.766 Hz along Z.
	Case 4 and Case 6	1.53 Hz along X; 1.55 Hz along Z.
First mode frequency of ES 'ω_s' (bare RC frame)	Case 2	1.14 Hz along X; 1.195 Hz along Z.
Central frequency considered for design of TSWD		1.47 Hz along X; 1.48 Hz along Z
Maximum displacement 'D_o' at roof level	Case 2	15.4 mm along X; 15.1 mm along Z.
	Case 6	15.11 mm along X; 14.74 mm along Z.
Maximum permissible displacement 'D_r' at roof level (with 25% response reduction after retrofitting)		11.55 mm along X; 11.33 mm along Z.

The story drifts and deformed shape of ES under seismic loading are shown in Figure 5. The existing structure is not showing any visible signs of distress. It is inferred that, with present stress condition, the structure is within elastic limits as considered in design. For conditions of Case 1, the column A5 (refer Figures 3 and 4) is worst stressed. The maximum column stresses obtained from the analysis have been normalised with respect to maximum column stress of A5 of Case 1, as tabulated in the Table 7.

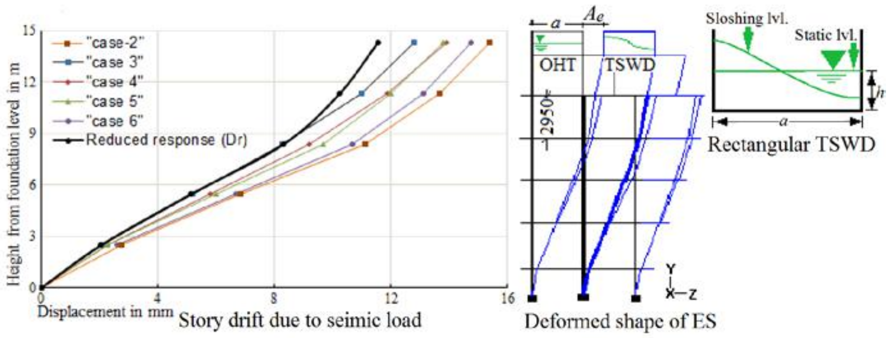

Fig. 5 Displacement of structure under different load cases along Z axis

Table 7: Normalised Column Stresses for All Structural and Loading Conditions

Col. no.	A1	B1	C1	A2	B2	C2	A3	B3	C3	A4	B4	C4	A5	B5	C5
Case 1	0.39	0.64	0.67	0.5	0.9	0.75	0.51	0.59	0.69	0.57	0.61	0.68	1	0.74	0.65
Case 2	0.87	0.93	1.16	1.02	1.15	1.04	1.01	1.09	1.08	1.05	1.15	1.19	**1.74**	1.19	1.17
Case 3	0.42	0.59	0.61	0.47	0.83	0.81	0.48	0.6	0.76	0.56	0.6	0.63	**1.01**	0.73	0.71
Case 4	0.48	0.67	0.68	0.57	0.87	0.88	0.55	0.7	0.79	0.66	0.66	0.74	**1.11**	0.82	0.77
Case 5	0.48	0.69	0.7	0.54	0.96	0.94	0.56	0.69	0.87	0.65	0.7	0.72	**1.18**	0.84	0.82
Case 6	0.55	0.78	0.78	0.66	1	1.01	0.63	0.81	0.92	0.75	0.77	0.85	**1.34**	0.94	0.88

For the bare RC frame in seismic condition (Case 2), 26 out of 30 columns have exceeded the column stresses of A5 of static condition (Case 1). If all the masonry panels are contributing as diagonal strut (Case 3), then the column stresses are of the same order as in Case 1.

Present study presumes that with less than 0.1% story drift the 230 mm masonry panels shall contribute as diagonal struts (Case 4). A 25% reduction of displacement response of Case 2 shall result in the story drift of <0.1%. This 25% reduced displacement is less than that of Case 4; hence stresses will also be lesser than that of Case 4 which are well within factor of safety considered in design.

RETROFITTING OF EXISTING STRUCTURES WITH TSWD SYSTEMS

Existing structures can be retrofitted by rigidly attaching a TSWD system with it.

1. Retrofitting with Single Frequency TSWD (STSWD)

The ES is retrofitted by rigidly attaching a TSWD of mass m_d , frequency ω_d and damping ratio ξ_d , with it as shown in Figure 6.

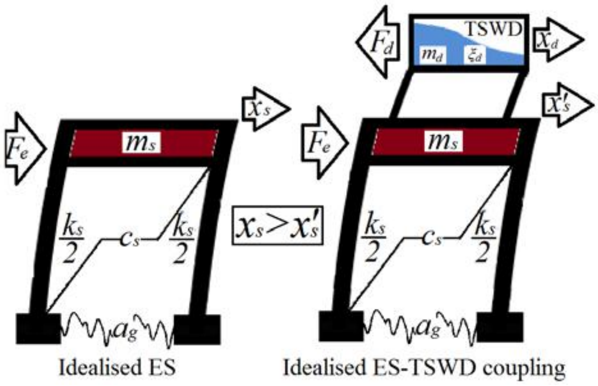

Fig. 6 Structure coupled withTSWD

The ES is assumed as single degree of freedom system (SDOF) of its first mode frequency ω_s , with which major part of its mass participates in the vibration. The structural deformation of this SDOF is governed by its damping ratio ξ_s and presented as dynamic magnification factor (DMF_o):

$$DMF_o = 1/2\,\xi_s \tag{1}$$

The ES-TSWD coupling behaves as two degree of freedom system. The dynamic magnification factor (DMF_r) of ES-TSWD coupled structure, subjected to harmonic excitation, is (Yu, 1999):

$$DMF_r = \frac{1}{\sqrt{RE^2 + IM^2}} \tag{2}$$

here

$$RE = 1 - \beta^2 - \mu\beta^2 \frac{f^2\left\{f^2 - \beta^2 + (2\xi_d\beta)^2\right\}}{(f^2 - \beta^2)^2 + (2f\xi_d\beta)^2} \tag{2a}$$

$$IM = 2\xi_S\beta + \frac{2\mu f\xi_d\beta^5}{(f^2 - \beta^2)^2 + (2f\xi_d\beta)^2} \tag{2b}$$

$\beta = \omega_e/\omega_s$, Frequency ratio,

$\mu = m_d/m_s$, Mass ratio,

$f = \omega_d/\omega_s$, Tuning ratio,

ω_e=Frequency of excitation,

The equivalent damping ratio 'ξ_e' of ES-TSWD coupled structure may be derived as:

$$\xi_e = \frac{1}{2(DMF_r)} \tag{3}$$

The ξ_e of a retrofitted structure depends on f, μ, β, ξ_s and ξ_d. For an accurately assessed ES, the ES-TSWD coupling is optimal if $\omega_d = \omega_s$. The response of the ES can be controlled through TSWD parameters ω_d, ξ_d, and μ.

The TSWD parameters can be determined from empirical equations, for a condition, that A_e is equal to the displacement of the host structure at the location of TSWD. The mass (m_d) of sloshing water in a TSWD is determined as (Ibrahim, 2005):

$$m_d = m_T\left[8\left(\frac{a}{h}\right)\frac{\tanh\{(2n-1)\pi h/a\}}{(2n-1)^3\pi^3}\right] \tag{4}$$

The required damping mass M_d for response reduction is large enough to be accommodated in a single TSWD. Thus, N number of TSWDs of same frequency for making a STSWD system is provided such that:

$$M_d = Nm_d \tag{5}$$

The design of the optimal TSWD systems for existing buildings is difficult, due to many approximations involved in assessment of condition of the existing structures with respect to mutual coherence between design idealisations and actual execution. Further, the TSWD properties are dependent on amplitude of excitation (A_e) of TSWD which is equal to the displacement of the host structure at the mounting location of TSWD and cannot be predetermined for broad band excitations. These approximations may lead to mistuning between ES and TSWD resulting in poor performance of retrofitting system.

2. Multiple Frequency TSWDs (MTSWD)

The MTSWD systems have been devised for structures of multiple degrees of freedom. The present study proposes MTSWD system in coupling with ES of approximately assessed dynamic properties against broad band excitations. The ES to be retrofitted is represented as a single degree of freedom (SDOF) system and the retrofitting device is multiple frequency TSWD system as shown in Figure 7.

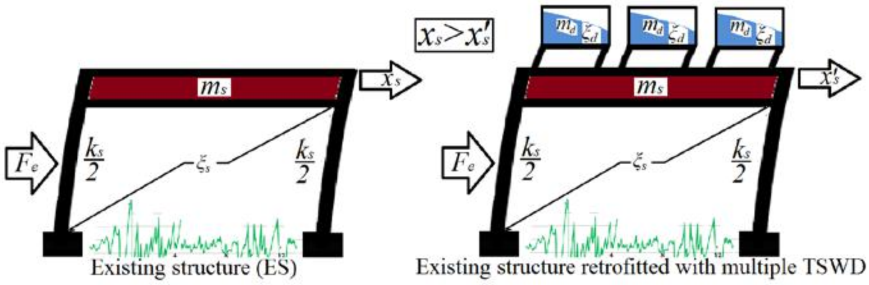

Fig. 7 Multiple frequency tuned sloshing water dampers (MTSWD) attached to SDOF structure

The equations of motion of the SDOF-MTSWD system contain several parameters that govern the performance of response control system. These parameters are:

n = total number of TSWD frequencies (generally odd number such as 3, 5 7….)

μ_{total} = ratio of the total sloshing mass of water in n TSWDs to the structural mass

μ_{kl} = ratio of the sloshing mass of water in one TSWD to the structural mass

ξ_s = damping ratio of the structure

ξ_d = damping ratio of the damper

ω_s = natural frequency of the structure (central frequency of MTSWD system)

ω_1 = natural frequency of the 1^{st} TSWD (lowest frequency of the ES)

ω_n = natural frequency of the n^{th} TSWD (highest frequency of the ES)

ω_k = natural frequency of the individual $\left(k^{th}\right)$ TSWD

ω_e = excitation frequency

f_k = tuning ratio of k^{th} TSWD with structural natural frequency $\left(\omega_k/\omega_s\right)$

f_{centre} = tuning ratio of central frequency TSWD with ω_s $\left(\omega_{\{(n+1)/2\}}/\omega_s\right)$

β = frequency ratio of excitation frequency to structural frequency $\left(\omega_e/\omega_s\right)$

FR = frequency range of TSWDs, (ω_1 to ω_n)

The frequencies of the TSWDs are equally spaced in the range FR. The equation of motion of the system shown in Figure 7 may be solved for forced harmonic excitation leading to steady state solution for structural displacement 'x_s' as (Park and Reed, 2001):

$$x_s = \frac{F_e}{m_s\omega_s^2}\left[\frac{1}{RE+IM}\right] \tag{6}$$

here

$$RE = 1-\beta^2-\sum_{k=1}^{n}\ \mu_k\beta^2\,\frac{\left(\mu_k\beta^2\right)f_k^2\left\{f_k^2-\beta^2+\left(2\xi_d\beta\right)^2\right\}}{(f_k^2-\beta^2)^2+(2\,f_k\xi_d\beta)^2} \tag{6a}$$

and

$$IM = 2\xi_s\beta+\sum_{k=1}^{n}\frac{2\mu_k\,f_k\xi_d\beta^5}{(f_k^2-\beta^2)^2+(2\,f_k\xi_d\beta)^2} \tag{6b}$$

The dynamic magnification factor (DMF_r) and effective damping ratio of retrofitted system may be expressed as Equations (2) and (3).

The MTSWD system may be designed with TSWDs of different frequencies spaced within the defined frequency range (FR) from the assessed frequency of the ES considered as central frequency. The total damping mass is distributed among these TSWDs of different frequencies.

2.1 Mass ratio distribution for MTSWDs

Two types of damping mass ratio distribution are considered for MTSWDs:

a) Uniformly distributed mass ratio (UDMR): The total sloshing water mass is equally divided among the regularly spaced frequency TSWDs, such that:

$$\mu_k = \frac{\mu_{total}}{n} \tag{7}$$

The UDMR is more effective under harmonic excitation for reducing the peak DMF of structure with multiple degrees of freedom.

b) Linearly distributed mass ratio (LDMR): The central frequency TSWD is provided with the highest sloshing mass which linearly decreases towards both ends. The LDMR is more robust to mistuning of TSWD with host structure.

Both the systems exhibit similar performance under broad band excitations. The present experimental study has been conducted with MTSWD system having LDMR.

SIMULATED EXPERIMETS

The retrofitting proposal has been examined through a sequence of simulated experiments on scaled model (SM) of ES, in coupling with real life sized STSWD and MTSWD systems, on shake table. The similitude requirements have been satisfied within available laboratory resources.

1. Geometrical Scaling

A linear reducing scale factor SL=20 has been applied to each linear dimension of the ES to accommodate the SM on the shake table. The geometrical parameters such that plan aspect ratio, elevation aspect ratio about axes, number of structural members and number of joints of SM are kept as SM≡ES. The respective dimensions of ES and SM are tabulated in Table 8.

Table 8: Linear Dimensions of ES and SM

Dimensional Feature	ES (mm)	SM (mm)
Overall plan dimensions	26500 x 8490	1325x 424.5
Bay width along Z	3530	176.5
C/c column spacing along X	2930	146.5
Stair bay width	2830	141.5
Beam projection from col. face	600	30
Foundation depth	2500	125
Floor to floor height	2950	147.5
Foundation to roof	14300	715
Height of OHT from roof	2600	130

2. Material Scaling and Cross Sectional Area of Structural Members of SM

The gross characteristics strength of ES, based on cross sectional area contribution of column and masonry compressive strut with their respective strengths, is 15.45 MPa (Shedid, 2006). The members of SM with scaling factor of 20 cannot be constructed in the ES material. Mild steel with characteristic yield strength of 250 MPa has been chosen as construction material for SM. Material scale factor 'MF' defined as the ratio of yield strength for mild steel of SM and characteristics strength of concrete-masonry composite of the ES is 16.18 (Sabnis et al. 1983). The required cross section area of structural members of SM is calculated as:

$$A_{SM} = \frac{A_{ES}}{(MF)(SL)^2} \tag{8}$$

For a typical concrete column of 250mm x 350mm of ES the column section required in the SM was 13.52 sq.mm in mild steel.

3. Dynamic Similitude Between ES and SM

The responses of a structure against dynamic excitations depend upon its frequency and damping ratio. The targeted similitude with respect to dynamic properties is SM≡ES.

The dynamic properties of ES in laboratory have not been scaled. The frequency of the SM was fine-tuned by varying the mass distribution among the floors. Desired damping is achieved by manipulating the tightness of mass attachments with the floors of the SM. The frequency of SM≡ES and the damping ratio of SM≡ES≈3% have been realised during the experiments. For all the structural conditions of the ES (Table 5), the simulated SMs of different frequency have been developed, from same fabricated skeleton, by manipulating and fine tuning the floor mass distribution.

4. Excitation and Displacement Response Scaling

The TSWD parameters are dependent on amplitude of excitation 'A_e' which is equal to the displacement response of host structure at its location. The equivalence of displacement response in prototype (ES) and model (SM) has been maintained. All the tests have been conducted for a displacement range of 16mm ('D_o') to 11mm ('D_r').

The North-South (N-S) and East-West (E-W) components of the acceleration time-histories recorded at the El Centro during the 1940 Imperial Valley earthquake (Chopra, 1995) has been considered two independent excitations. An artificial time history, consistent with the BIS: 1893 response spectrum, designated as BIS: 1893 compatible, has also been considered (Sharma et. al 2012; Levy and Wilkinson, 1976; Mukharjee and Gupta, 2002).). The excitation amplitudes have been scaled to cause maximum displacement of 15mm (approximately) at roof level of SM. These excitation intensities have been considered as bench mark intensities.

5. Similitude Requirements of TSWD

The real TSWDs required for retrofitting application of ES has been tested on the shake table.

6. Similitude Requirements of Retrofitted ES and SM-TSWD Coupling

There is no scaling of dynamic properties and displacement response of ES with respect to that of SM. For a fixed set of parameters, the performance of TSWD retrofitting system is dependent on mass ratio. The SM-TSWD coupling performance can be replicated as ES-TSWD coupling (representing retrofitted ES) in real life by maintaining the mass ratio equivalence. The mass ratios observed during the experiments can be achieved in real life by installing appropriate number of TSWDs on ES (Equation 5).

SCALED MODEL, TSWD AND LABORATORY TEST SETUP

The frequency of ES is almost equal along both the principal axes. The SM was fabricated with 4 mm diameter MS wires of cross sectional area 12.56 mm^2 (as against calculated 13.52 mm^2) representing columns. Horizontal members were made of 8 mm diameter rods as beams. The self-weight of the SM is 39 kg. The imposed loads have been applied through attaching lead blocks and MS blocks of different sizes. The fine tuning of the dynamic properties is accomplished by manipulating floor load distribution. Symmetry of loading about line of symmetry has been maintained. The SM has been bolted rigidly on a unidirectional shake table.

Two sets of TSWDs have been constructed by 4 mm thick acrylic sheet. The freeboard for the tanks have been decided through IITK-GSDMA guidelines for seismic design of liquid storage tanks (Jain and Jaiswal, 2007). In zone III, for 370 mm tanks, the maximum sloshing wave height is calculated as 37 mm. Minimum 40 mm freeboard has been provided during all the shake table tests.

First set of 3 acrylic boxes, of internal dimensions 145 mm (along X) x 370 mm (along Z) in plan and 120 mm depth, have been made. These boxes have been used as TSWDs up to 80 mm water depth, for experimental tests along Z axis only with 145 mm side kept normal to the direction of vibration. Second set of 3 acrylic boxes of internal dimensions 370 mm x 370 mm in plan and 200 mm depth have been constructed for observing response reducing performances of TSWDs along both the principal axes. The 200 mm boxes have also been used for verification and extension of the observations to the large sized TSWDs of 160 mm depth. The sizes of these boxes have been manipulated by fixing polythene wrapped foam pieces of desired thickness on the inner face of the walls.

One box is fixed on the four central columns extended from main frame to simulate OHT in ES and designated as TL-1. The remaining two boxes are placed on the roof, one on each side of axis of symmetry, designated as locations TL-2 and TL-3 as has been sketched in Figure 8.

The laser displacement sensor was fixed, on a card board, at the base level of TSWD at location TL-1, for recording the displacements during all tests.

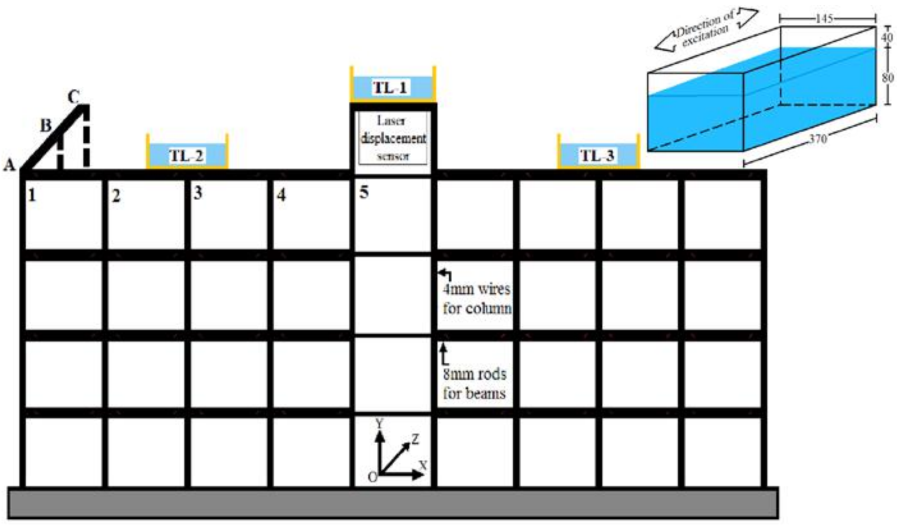

Fig. 8 Structural Skeleton of Scaled Model (SM)

EXPERIMENTAL PROGRAMME

The testing protocol was focussed on displacement response of the structure under different types of dynamic excitations. The SM and TSWDs have been subjected to a sequenced series of dynamic load tests, on shake table, in five stages with free and forced excitations as mentioned in Table 9.

Table 9: Experimental Test Matrix

Excitation Type	Intended Observation
Free vibration	On bare SM, for consistency of SM and frequency observations
Free vibration	On SM-TSWD coupling, for determination of optimum TSWD parameters.
Forced harmonic excitation	On bare SM, for obtaining suitable test regime and range of base excitation (A_{be}). (For obtaining bench mark excitation intensity).
Forced broad band excitation	
Forced harmonic excitation	On SM-TSWD coupling, for visualisation of response reduction due to single frequency TSWD (STSWD) and effect of mass ratio.
Forced broad band excitation	
Forced harmonic excitation	On SM-TSWD coupling, for visualisation of response reduction due to multiple frequency TSWD (MTSWD). Performance observation.
Forced broad band excitation	

The performance of TSWD system has been verified and substantiated along both the principal axes. First the experiments have been conducted with excitations along the Z axis of the SMs. The symmetry of sloshing mass about the axis of symmetry of SM was maintained during all the tests along Z axis. Subsequently the text matrix of Table 9 was repeated with the SM oriented by 90^o such that X axis of the SM is parallel to direction of vibration. The test run durations have been kept 16 to 22 seconds for observing minimum 25 structural vibration cycles. The recorded observations are mean of 5 test runs in each configuration/setting. The displacement response parameters of TSWD systems in coupling with SMs with respect to mass ratios have been observed.

1. Floor Mass Distribution and Frequency of SM

The Bare SM (no water in TSWDs) tests have been conducted for determining the floor wise mass distribution for desired frequency. The SM is subjected to initial displacement of the order of 11 mm at roof level and allowed to oscillate. The SM frequencies recorded by laser displacement sensor and corresponding floor wise mass distributions are mentioned in Table 10.

Table 10: Floor Mass Configuration and Frequency of SM by Free Vibration Tests

Test Id	SM ID	Floor Load Distribution						Observed SM frequency (Hz)
		Gr. flr. UDL (kg/m)	1st flr. (kg)	2nd flr. (kg)	3rd flr. (kg)	Roof (kg)	Total (kg)	
Along ‘Z’ axis								
4	SM_4	1.2	108	108	108	37	413	1.76
6	SM_5	1.2	152	134	118	86	542	1.48
8	SM_6	1.2	100	152	152	152	608	1.2
Along ‘X’ axis								
99	SM_{x1}	1.2	100	100	100	40	392	1.8
100	SM_{x2}	1.2	134	134	134	88	502	1.47
101	SM_{x3}	1.2	152	152	152	132	640	1.14

These tests demonstrate the consistency of structural behaviour of SM under dynamic excitations. SM_4 and SMx_1 represent ES with structural contribution of all the masonry panels. SM_6 and SM_{x3} represent the state of no structural contribution of masonry panel. The real condition of ES will be within these extreme conditions of frequency range of 1.14 Hz to 1.80 Hz, such as SM_5 or SM_{x2}. The vibration amplitude decay, during the free vibration tests on bare SMs, exhibits a damping ratio of the order of 0.75%.

2. Optimum Size Search of TSWD with Respect to SM

The optimum length 'a' of the TSWDs has been searched for 40 mm, 80 mm and 160 mm depths in coupling with SMs of different frequencies with water in TSWD at TL-1 location. The sizes have been appropriated by inserting polythene wrapped foam pieces. An initial displacement of approximately 11 mm has been given to SM at the base of TSWD as amplitude of excitation 'A_e'. The length of TSWD causing fastest amplitude decay has been considered optimum for corresponding SM, exhibiting maximum effective damping ratio of SM-TSWD coupling.

The dimensions of TSWDs along Z axis have been searched with 145 mm x 370 mm acrylic box. The operations have been repeated with SM_4, SM_5 and SM_6 for respective optimum lengths of TSWDs for 1.76 Hz, 1.48 Hz and 1.2 Hz frequencies of structure. The effective damping ratio observations are mentioned in Table 11.

Table 11: Free Vibration Observations on SM-TSWD Coupling Along Z axis

Test Id/ Trial no.	SM Id	TSWD Size			Vibration Amplitude of SM-TSWD (mm)				Mass ratio 'μ' (%)	Effective damping ratio 'ξ_e' (%)
		Length 'a' (mm)	Sloshing mass 'm_d'(kg)	TSWD(Length 'a' x Depth 'd') Id	Initiation		End			
					Cycle no.	Amplitude	Cycle no.	Amplitude		
9/iv	SM_4	235	1.63	$TSWD_{235x80}$	2	11.05	25	1.66	0.39	1.31
10/iv		185	0.76	$TSWD_{185x40}$	2	10.9	25	2.55	0.18	1.00
12/iv	SM_5	280	2.1	$TSWD_{280x80}$	2	11.85	24	1.49	0.39	1.50
13/iv		220	0.93	$TSWD_{220x40}$	2	11.36	24	2.77	0.17	1.02
15/iii	SM_6	360	2.92	$TSWD_{360x80}$	3	11.95	23	1.38	0.48	1.72
16/iv		265	1.16	$TSWD_{265x40}$	3	11.45	25	2.24	0.19	1.18

The dimensions of TSWDs along X direction have been searched with 370 mm x 370 mm acrylic box at TL-1 location of for 80mm water depth only. The TSWD sizes normal to axis of vibration has been kept as 235 mm for SM_{x1}, 280 mm for SM_{x2} and 360 mm for SM_{x3}.

The optimal lengths of TSWDs for SM_{x1}, SM_{x2} and SM_{x3} along with the already determined optimal TSWD lengths along the Z axis gives the optimal length of TSWDs along both the axes. Thus, three sizes of the TSWDs have been obtained for three structural conditions as mentioned in Table 12.

Table 12: Parameters of Optimal TSWDs of 80 mm Water Depth Along Both the Principal Axes

Test Id	Structural Condition	Dimensions of TSWD (mm)		Sloshing Mass (kg)	TSWD Id
		Along Z	Along X		
102	Walls acting as diagonal strut (SM_4 & SM_{X1})	235	230	2.56	$TSWD_{230x235}$
103	Intermediate condition (SM_5 & SM_{X2})	280	285	4.13	$TSWD_{285x280}$
104	No structural contribution of walls (SM_6 & SM_{X3})	360	370	7.62	$TSWD_{370x360}$

The size searches for large TSWDs with 160mm water, designated as $TSWD_{160}$, have been conducted along X and Z directions. The large size TSWD experiments have been conducted for SM_4, SM_5, SM_{x1} and SM_{x2} only with single acrylic box of 370 mm x 370 mm x 200 mm size fixed at TL-1. The optimal lengths of the $TSWD_{160}$, have been recorded in Table 13.

Table 13: Parameters of 160mm deep optimal TSWDs along both the principal axes of ES

Test Id	Structural Condition	Dimension of TSWD(mm)		Sloshing mass (kg)	TSWD Id
		Along Z	Along X		
121	Walls acting as diagonal strut (SM_4 and SM_{X1})	275	280	5.26	$TSWD_{275x280x160}$
124	Intermediate condition (SM_5 and SM_{X2})	350	350	9.88	$TSWD_{350x350x160}$
	No structural contribution of walls (SM_6 and SM_{X3}) determined from equations available in literature	455	490	21.77	$TSWD_{455x490x160}$

For an intermediate condition of the structure, the typical optimum size search observations with 80 mm water depth TSWD and 160 mm water depth TSWD are shown in Figure 9.

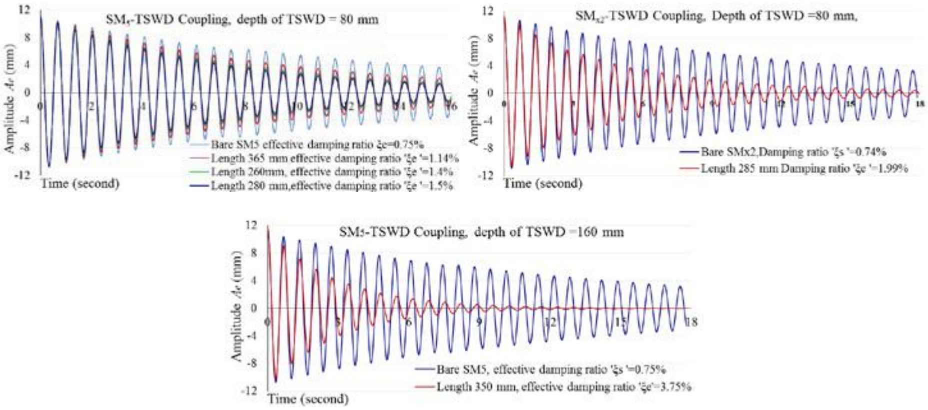

Fig. 9 Size search observations for intermediate structural condition of ES coupled with optimal TSWDs

3. Bench Mark Excitation Intensities at Base of Bare SMs for Test Regime

The retrofitting strategy is focused on reducing the maximum displacement from D_o (15.4 mm) to D_r (11.55 mm). The forced vibration tests have been conducted for determining the intensities of the excitations at the base of bare SMs causing a displacement response of approximately 15 mm at the location TL-1. These excitation intensities have been considered as bench mark excitation.

3.1 Resonant Harmonic Excitations

The resonant harmonic excitations of 0.75 mm and 1.0 mm at base $\left(A_{be}\right)$ have caused the maximum displacements of 11 mm to 15 mm. The observed maximum displacements at the base level of TL-1 and corresponding damping ratios are given in Table 14.

Table 14: Bare SM Subjected to Resonant Harmonic Excitation

SM Id	Test Id/ Trial no.	Amplitude of Excitation at Base A_{be} (mm)	Displacement at TSWD Base A_e (mm)	Damping Ratio (%)
SM4	20/iii	0.75	12.66	2.96
	20/iv	1	15.96	3.13
SM_5	21/iii	0.75	12.24	3.06
	21/iv	1	15.75	3.17
SM_6	22/iii	0.75	12.03	3.12
	22/iv	1	15.36	3.26
SM_{x1}	105	0.75	12.25	3.06
	106	1	15.63	3.2
SM_{x2}	107	0.75	11.92	3.14
	108	1	15.38	3.25
SM_{x3}	109	0.75	11.72	3.2

	110	1	14.94	3.34

3.2 Broad band excitations

The bare SMs have been subjected to broad band excitations at the base, through shake table for intensities from 0.032 g to 0.1 g, increased in small incremental steps. The excitation amplitudes causing maximum displacement of approximately 15 mm at the base of TL-1have been given in Table 15. The bench mark excitation intensities obtained along Z axis have been applied along X axis also.

Table 15: Bare SM Subjected to Broad Band Ground Motion Time Histories

SM Id	Excitation Id	Test Id	Excitation amplitude at base 'g'	Displacement at TL-1(mm)
SM_4	El Centro (N-S)	65b	0.064g	16.84
	El Centro (E-W)	66b	0.07g	15.89
	BIS:1893	67b	0.1g	14.64
SM_5	El Centro (N-S)	68b	0.064g	14.65
	El Centro (E-W)	69b	0.07g	16.23
	BIS:1893	70b	0.075g	14.55
SM_6	El Centro (N-S)	71b	0.04g	14.92
	El Centro (E-W)	72b	0.044g	16.08
	BIS:1893	73b	0.06g	13.39

RETROFITTING PERFORMANCE OBSERVATIONS OF TSWDS

The rigidly mounted acrylic boxes at the locations, TL-1, TL-2 and TL-3, have been converted into TSWDs of desired frequency, having 40 mm, 80 mm and 160 mm water depths, by manipulating the sizes. The behaviour of SM-TSWD couplings have been observed against dynamic excitations.

1. SM Coupled with Optimal TSWDs Subjected to Resonant Harmonic Excitations

The SMs coupled with respective frequency TSWDs forms an optimal SM-STSWD system. The mass ratio variations (from 0.17% to 2.44%) for each coupling have been achieved by different combinations of the TSWDs. Each optimal SM-STSWD combination was first subjected to resonant harmonic base excitation of 0.75 mm amplitude subsequently the process was repeated with 1.0 mm amplitude. The observations of SM-TSWD couplings oriented along Z and X axes are presented in Table 16.

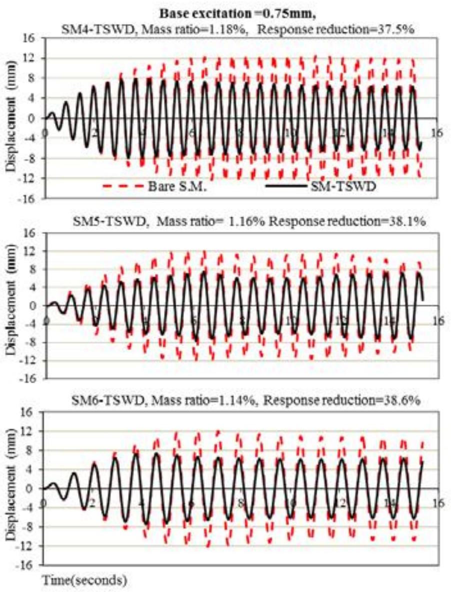

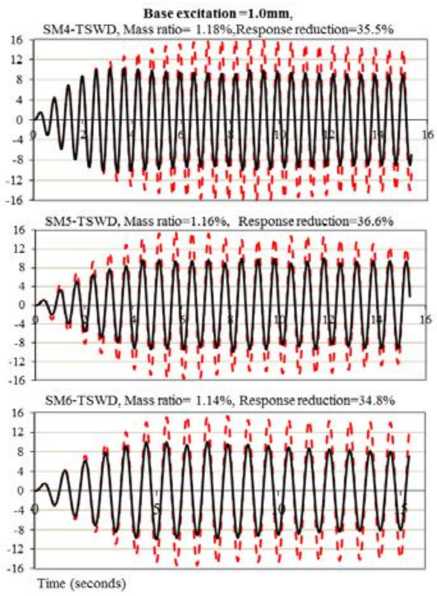

Fig. 10 SM_4, SM_5, SM_6 with optimal TSWDs subjected to resonant harmonic excitation

Table 16: Performance of SM-TSWD Coupling Subjected to Forced Harmonic Excitation

TSWD Combination		Mass Ratio μ (%)	Experimental Observations							
			$'A_{be}'$ =0.75 mm				$'A_{be}'$ =1.0 mm			
At TL-1	At TL-2 and TL-3		Test Id	Displacement Response(mm) Max.	Displacement Response(mm) % Red.	Effective Damping Ratio 'ξ_e' (%)	Test Id	Displacement Response(mm) Max.	Displacement Response(mm) % Red.	Effective Damping Ratio 'ξ_e' (%)
SM4 coupled with optimal TSWDs, subjected to resonant excitation of 1.76 Hz										
No TSWD	No TSWD	0	20/iii	12.66	0	2.96	20/iv	15.96	0	3.13
$TSWD_{185x40}$	No TSWD	0.18	25	11.69	7.66	3.21	26	14.89	6.7	3.36
$TSWD_{235x80}$	No TSWD	0.39	27	10.5	17.06	3.57	28	13.46	15.66	3.71
$TSWD_{235x80}$	$TSWD_{185x40}$	0.76	31	9.11	28.04	4.12	32	11.73	26.5	4.26
$TSWD_{185x40}$	$TSWD_{235x80}$	0.97	33	8.9	29.7	4.21	34	11.54	27.69	4.33
$TSWD_{235x80}$	$TSWD_{235x80}$	1.18	35	7.91	37.52	4.74	36	10.3	35.46	4.85
SM5 coupled with optimal TSWDs, subjected to resonant excitation of 1.48 Hz										
No TSWD	No TSWD	0	21/iii	12.24	0	3.06	21/iv	15.75	0	3.17
$TSWD_{220x40}$	No TSWD	0.17	37	11.04	9.8	3.4	38	14.71	7.83	3.4
No TSWD	$TSWD_{220x40}$	0.34	39	10.42	14.87	3.6	40	13.89	12.97	3.6
$TSWD_{220x40}$	$TSWD_{220x40}$	0.52	41	9.61	21.49	3.9	42	13.16	17.54	3.8
No TSWD	$TSWD_{280x80}$	0.77	43	8.5	30.56	4.41	44	11.79	26.13	4.24
$TSWD_{280x80}$	$TSWD_{280x80}$	1.16	45	7.58	38.07	4.95	46	9.99	37.41	5.01
No TSWD	$TSWD_{280x285x80}$	1.52	47	6.98	42.97	5.37	48	7.18	55.01	6.96
$TSWD_{280x285x80}$	$TSWD_{280x285x80}$	2.28	49	5.75	53.02	6.52	50	6	62.41	8.33
SM6 coupled with optimal TSWDs, subjected to resonant excitation of 1.2 Hz										
No TSWD	No TSWD	0	22/iii	12.06	0	3.11	22/iv	15.37	0	3.25
$TSWD_{265x40}$	No TSWD	0.19	51	10.91	9.54	3.44	52	14.13	11.47	3.54
No TSWD	$TSWD_{265x40}$	0.37	53	9.97	17.33	3.76	54	13.18	17.42	3.79
$TSWD_{265x40}$	$TSWD_{265x40}$	0.56	55	9.21	23.63	4.07	56	12.31	22.87	4.06
$TSWD_{360x80}$	$TSWD_{265x40}$	0.85	57	8.18	32.17	4.58	58	10.87	31.89	4.6
No TSWD	$TSWD_{360x80}$	0.96	59	7.7	36.15	4.87	60	10.27	35.65	4.87
$TSWD_{265x40}$	$TSWD_{360x80}$	1.14	61	7.4	38.64	5.07	62	10.02	37.22	4.99
$TSWD_{360x80}$	$TSWD_{360x80}$	1.44	63	6.58	45.44	5.7	64	8.84	44.61	5.66
SM_{x1} coupled with optimal TSWDs, subjected to resonant excitation of 1.8 Hz										
No TSWD	$TSWD_{230x235}$	1.3	111	7.83	38.15	4.79	112	10.02	37.22	4.99
$TSWD_{230x235}$	$TSWD_{230x235}$	1.94	113	6.30	50.24	5.95	114	8.52	46.62	5.87
SM_{x2} coupled with optimal TSWDs, subjected to resonant excitation of 1.47 Hz										
No TSWD	$TSWD_{285x280}$	1.63	115	6.52	46.73	5.75	116	8.43	46.48	5.93
$TSWD_{285x280}$	$TSWD_{285x280}$	2.44	117	5.26	57.03	7.13	118	6.89	56.25	7.26
SM_{x3} coupled with optimal TSWDs, subjected to resonant excitation of 1.14 Hz										

No TSWD	$TSWD_{370x360}$	2.35	119	5.39	55.31	6.96	120	6.78	55.89	7.37

The displacement response of SMs, in coupling with STSWD systems, for a mass ratio of approximately 1.15%, is less than 11 mm and response reduction is more than 30% for all structural conditions as shown in Figure 10.

These tests were optimal performance observations of STSWD systems against resonant dynamic excitations such that $f = 1$ and $\beta = 1$.

2. Mass Ratio and Effective Damping Ratio of SM-STSWD Coupling

The observed effective damping ratios of SM-STSWD couplings have been plotted with respect to mass ratio in Figure 11.

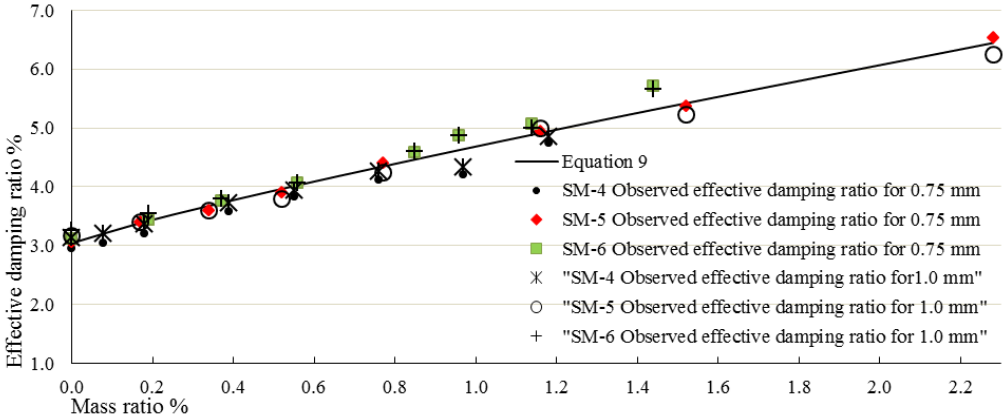

Fig. 11 Effective damping ratio of optimal SM-TSWD couplings (simulating retrofitted ES) subjected to resonant harmonic base excitation

The plot shows a consistent relationship between effective damping ratio 'ξ_e' and mass ratio 'μ' of SM-TSWD coupling. The relationship is expressed as:

$$\xi_e = \xi_s + \frac{5}{\xi_s}\left(\mu^{(\xi_s/5)^{0.25}}\right) \tag{9}$$

The unique number 5 in the RHS of Equation (9) is derived from the fact that 5% damping ratio is standard reference value in the codes. The equation captures the characteristics of STSWD systems that its effectiveness increases with increase in mass ratio and the system is more effective on structures with low damping.

The Equation (9) has been validated for large sized TSWD of 160 mm water depth in coupling with SM_4 and SM_5, against 'A_{be}' of 1.0 mm (Figure 12).

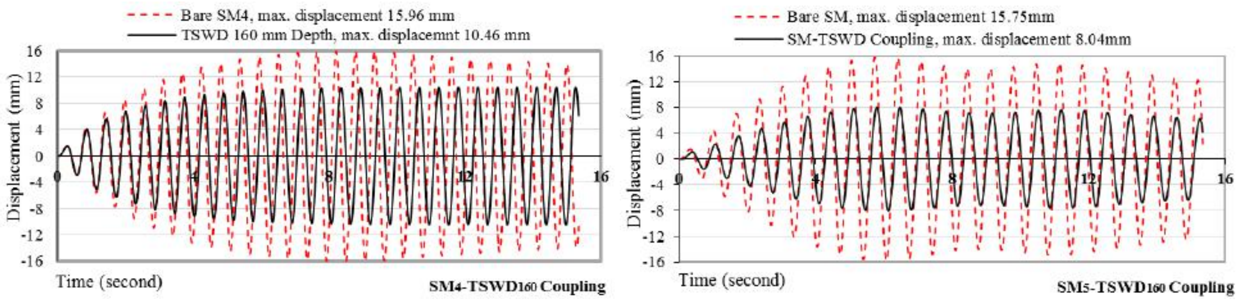

Fig. 12 SM_4–$TSWD_{275x280x160}$ and SM_5–$TSWD_{350x350x160}$ couplings subjected to harmonic excitation at base

The observations are tabulated in Table 17. The experimental values of 'ξ_e' closely follow the values calculated by Equation (9).

Table 17: 160 mm TSWD and SM Coupling Subjected to Forced Harmonic Excitation

SM Id	TSWD Id	Test Id	Total Water Mass (kg)	Sloshing Water Mass (kg)	Mass Ratio μ %	Max. Displacement	Effective Damping Ratio ξ_e (%)	
							Observed	From Eq. 9
SM_4	$TSWD_{275x280x160}$	122	12.32	5.26	1.24	10.46	4.78	5.06
SM_5	$TSWD_{350x350x160}$	125	19.6	9.878	1.76	8.04	6.22	5.78

3. Specific Mass Ratio

The efficiency of the TSWD system is expressed by effectiveness ratio 'E' as percentage structural response reduction due to incorporation of the retrofitting measure (Rai et al., 2011).

The mass ratio normalised with respect to effectiveness ratio gives specific mass ratio (μ_s) required for one percentage response reduction of the retrofitted structure with respect to un-retrofitted structure, expressed as:

$$\mu_s = \frac{\mu}{E} \tag{10}$$

Lesser is the specific mass ratio; more efficient is the TSWD based retrofitting system.

4. SMs Coupled with Optimal STSWD System Subjected to Broad Band Excitations

For broad band excitations, $\beta = 1$ cannot be realised. The tests have been conducted for optimal SM-STSWD couplings, with 80 mm water (approximately 1.15% mass ratio), subjected to the benchmarked broad band excitations for observing displacement response reduction. The displacements of optimal SM-$STSWD_{80}$ couplings, simulating retrofitted ES, have been compared with bare SM displacements in Figures 13, 14 and 15. The effectiveness ratio and specific mass ratio of the optimal SM-STSWD couplings subjected to different types dynamic excitations have been calculated in Table 18.

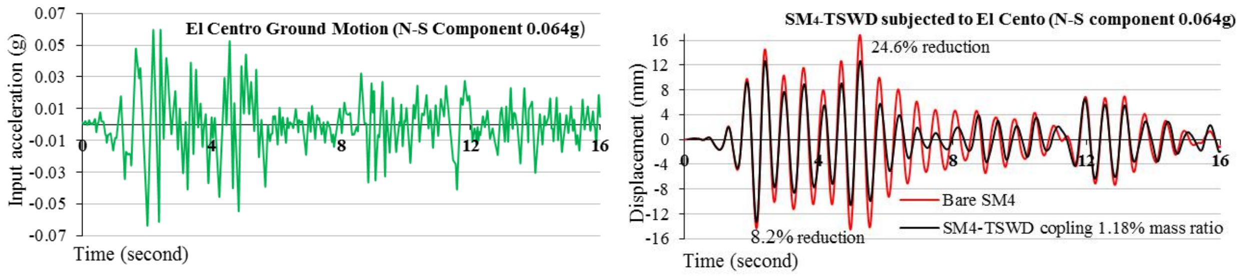

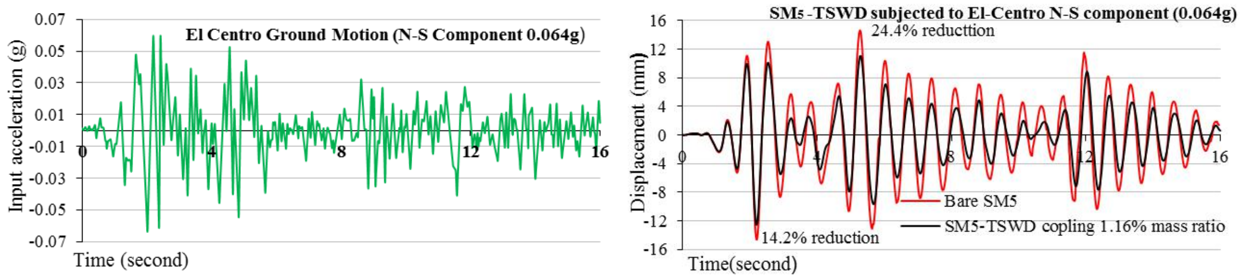

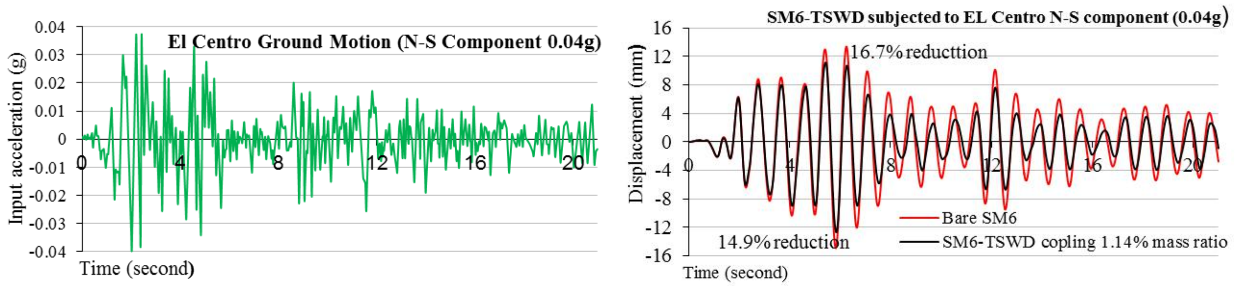

Fig. 13 SM-TSWD coupling subjected to El Centro ground motion (N-S component)

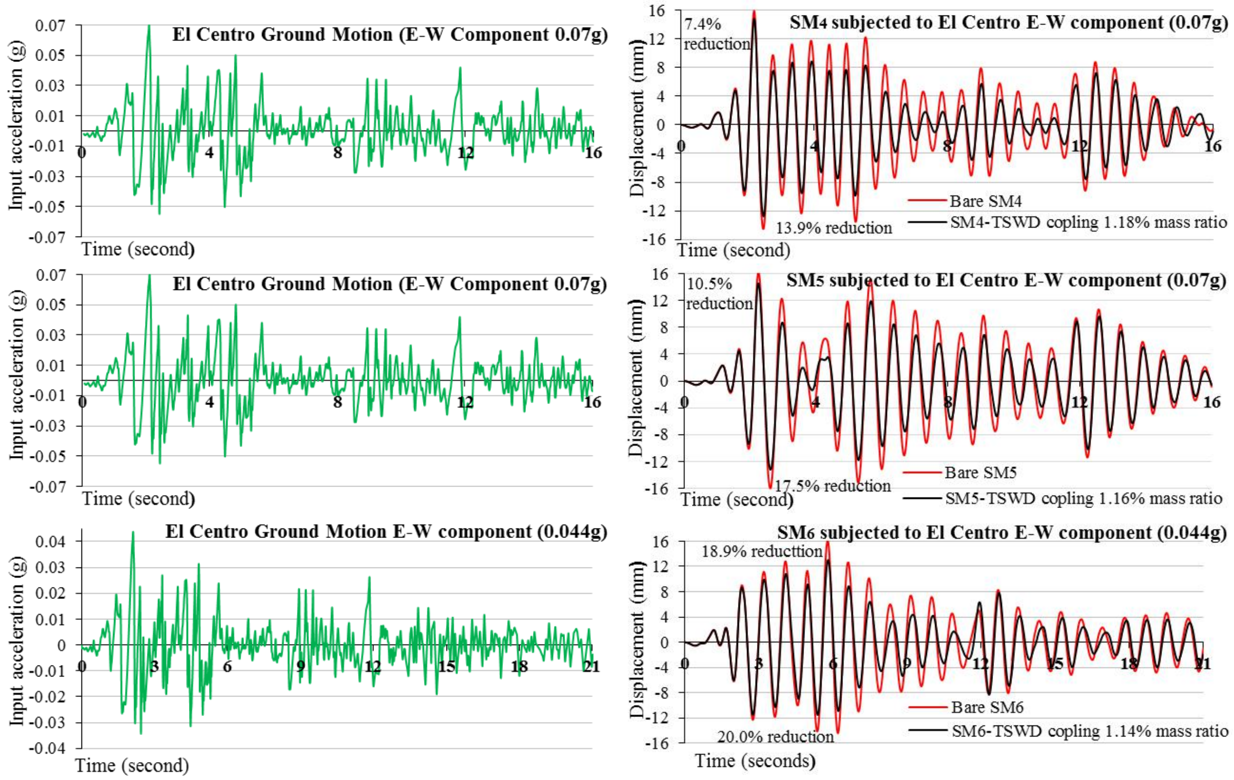

Fig. 14 SM-TSWD coupling subjected to El Centro ground motion (E-W component)

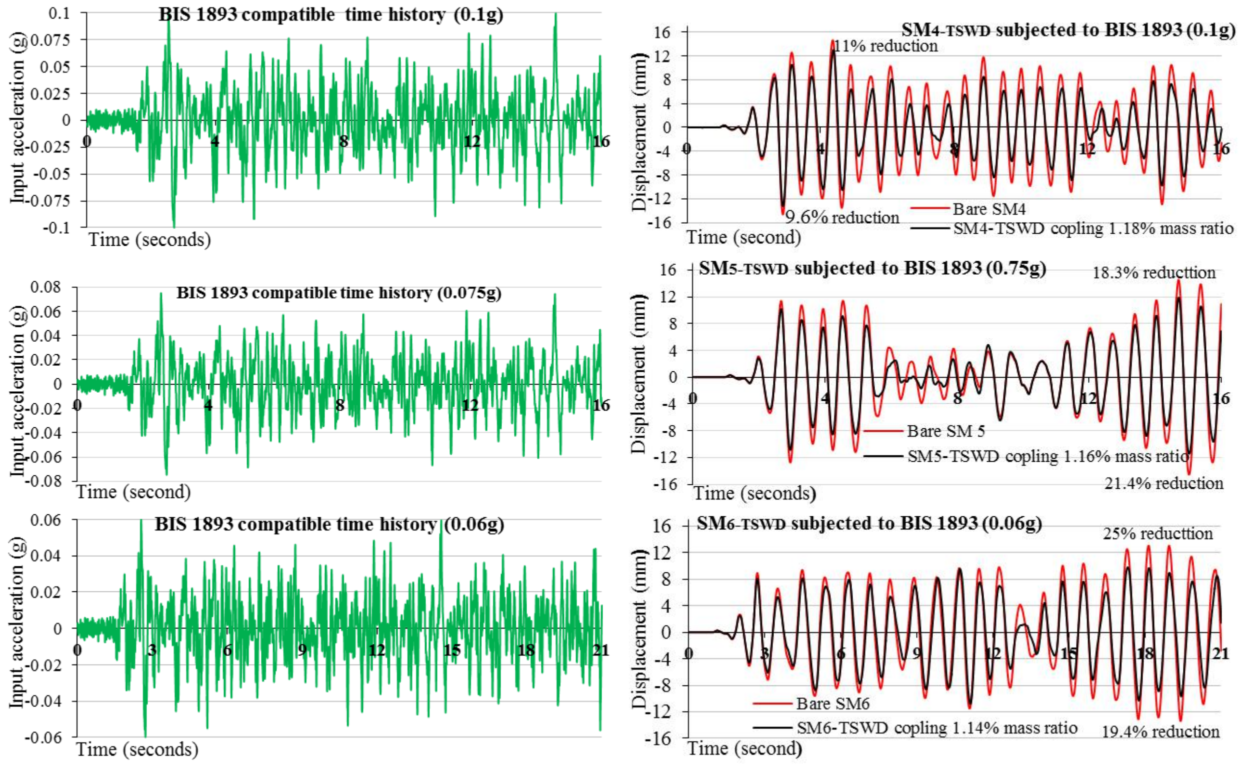

Fig. 15 SM-TSWD coupling subjected to BIS 1893 compatible time history

Table 18: Effectiveness Ratio and Specific Mass Ratio of Optimal STSWD Systems

Test ID	Excitation ID	Excitation Amplitude at Base	Maximum Displacement (mm)		Effectiveness Ratio *E* (%)	Specific Mass Ratio μ_s (%)
			Bare SM	SM-STSWD Coupling		
SM_4-TSWD coupling, total water mass 8.178 kg, sloshing mass 4.893 kg, mass ratio 1.18%						
20/iii	Harmonic 1.76 Hz	0.75 mm	12.66	7.91	37.52	0.0315
20/iv	Harmonic 1.76 Hz	1.0 mm	15.96	10.30	35.46	0.0333
65	El Centro (N-S)	0.064g	16.84	13.32	20.90	0.0565
66	El Centro (E-W)	0.07g	15.89	14.79	6.92	0.1705
67	BIS:1893	0.1g	14.64	13.23	9.63	0.1225
SM_5- TSWD coupling, total water mass 9.744 kg, sloshing mass 6.294 kg, mass ratio 1.16%						
21/iii	Harmonic 1.48 Hz	0.75 mm	12.24	7.58	38.07	0.0305
21/iv	Harmonic 1.48 Hz	1.0 mm	15.75	9.99	37.41	0.0365
68	El Centro (N-S)	0.064g	14.65	12.55	14.33	0.0809
69	El Centro (E-W)	0.07g	16.23	14.53	10.47	0.1107
70	BIS:1893	0.075g	14.55	11.89	18.28	0.0635
SM_6- TSWD coupling, total water mass 9.889 kg, sloshing mass 7.01 kg, mass ratio 1.14%						
22/iii	Harmonic 1.2 Hz	0.75 mm	12.06	7.4	38.64	0.0288
22/iv	Harmonic 1.2 Hz	1.0 mm	15.37	10.02	37.22	0.0323
71	El Centro (N-S)	0.04g	14.92	12.7	14.88	0.0766
72	El Centro (E-W)	0.044g	16.08	13.04	18.91	0.0603
73	BIS:1893	0.06g	13.39	10.79	19.42	0.0587

The response reductions with respect to bare SM displacements have been observed in all the SM-STSWD couplings with varied effectiveness. Total water mass contained in TSWDs in respective tests has been mentioned for evaluating water mass efficiency in the TSWD systems.

The effectiveness of the STSWD systems against broad band excitations is considerably less as compared to that against harmonic excitation. Against resonant harmonic excitation the maximum specific mass ratio (μ_s) is 0.0365 for optimal STSWD system, requiring 0.913% mass ratio for 25% response reduction. For the SM and optimal STSWD coupling subjected to broad band excitation the maximum value of (μ_s) is 0.1705 against, requiring 4.625% mass ratio for 25% response reduction exhibiting 80% efficiency loss of STSWD system against broad band excitations.

4.1 SM Coupled with Optimal 160 mm STSWD Subjected to Broad Band Excitation

Tests have also been conducted with 160 mm deep TSWDs in optimal coupling with SM_4 and SM_5 against BIS:1893 compatible broad band excitation for retrofitting performance observations. The observations are plotted in Figure 18 and evaluated in Table 19. The efficiency losses of STSWD system against broad band excitations have been observed.

Table 19: SM Coupled with Optimal 160mm Deep TSWD Subjected to BIS: 1893 Compatible Excitation

SM Id	TSWD Id	Excitation Intensity at Base	Mass Ratio μ %	Bare SM		SM-TSWD		Effective-ness Ratio *E* (%)	Specific Mass Ratio μ_s (%)
				Test Id	Max. Displacement	Test Id	Max. Displacement		
SM_4	$TSWD_{275x280x160}$	0.1g	1.24	67b	14.64	123	13.1	10	0.124

SM_5	$TSWD_{350x350x160}$	0.075g	1.76	70b	14.55	126	11.27	23	0.0765

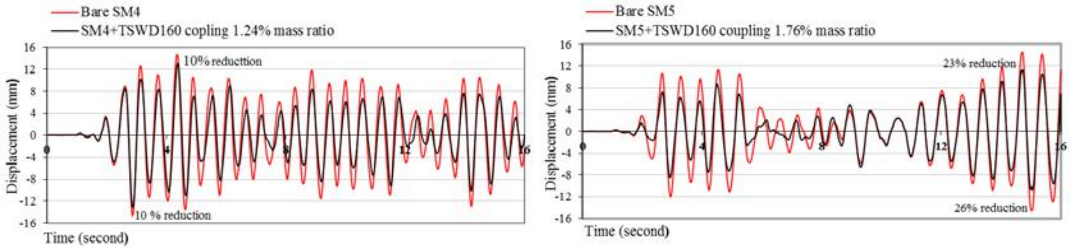

Fig. 16 SM_4-$TSWD_{275x280x160}$ and SM_5-$TSWD_{350x350x160}$ couplings subjected to BIS: 1893 compatible excitation

5. SMs Coupled with Optimal and Non-optimal STSWD System Subjected to Dynamic Excitations

A symmetrical STSWD system as shown in Figure 17, consisting of $TSWD_{280x80}$ at TL-1, $TSWD_{220x40}$ at TL-2 and TL-3 has been devised. This STSWD system is optimal with respect to SM_5 having a sloshing mass of 3.968 kg (μ=0.72%) and 23% detuned with respect to SM_4 and SM_6. The effect of detuning on response reducing performance of the STSWD system against different types of dynamic excitations has been evaluated through simulated experiments as recorded in Table 20.

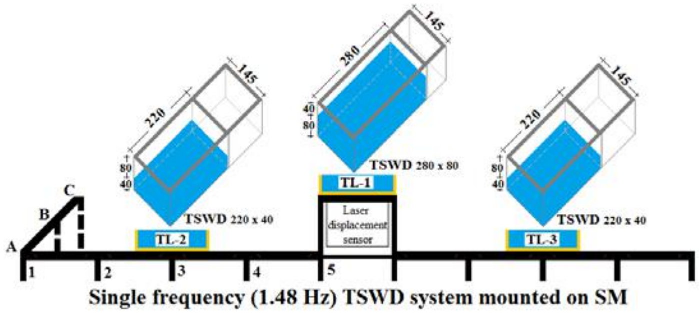

Fig. 17 Acrylic boxes converted as STSWD system

Table 20: STSWD System Coupled with SMs for Optimal and Non-Optimal Conditions

Test Setup	Excitation Definition		Max. Displacement				Effectiveness Ratio *E* (%)	Specific Mass Ratio μ_s (%)
	Identification	A_{be}	Bare SM 'D_o'		SM-TSWD 'D_r'			
			Test Id	D_o (mm)	Test Id	D_r (mm)		
SM_4-STSWD coupling; Mass ratio μ=0.95%	Harmonic 1.76 Hz	0.75 mm	20/iii	12.66	74	10.23	19.19	0.050
	El Centro (N-S)	0.064g	65-b	16.84	75	15.36	8.79	0.108
	El Centro (E-W)	0.07g	66-b	15.89	76	14.96	5.85	0.162
	BIS:1893 comp.	0.1g	67-b	14.64	78	13.81	5.67	0.168
SM_5-STSWD coupling; Mass ratio μ=0.72%	Harmonic 1.48 Hz	0.75 mm	21/iii	12.24	83	8.62	29.58	0.024
	El Centro (N-S)	0.064g	68-b	14.65	84	13.19	9.97	0.072
	El Centro (E-W)	0.07g	69-b	16.23	85	14.81	8.75	0.082
	BIS:1893 comp.	0.075g	70-b	14.55	86	12.59	13.47	0.053
SM_6-STSWD coupling;	Harmonic 1.2 Hz	0.75 mm	22/iii	12.06	91	10.62	11.94	0.054
	El Centro (N-S)	0.04g	71-b	14.92	92	14.12	5.36	0.121
	El Centro (E-W)	0.044g	72-b	16.08	93	14.55	9.51	0.068

Mass ratio μ=0.65%	BIS:1893 comp.	0.06g	73-b	13.39	94	12.51	6.57	0.099

The effect of detuning causing further efficiency loss of STSWD system against broad band excitations is evident from increased specific mass ratios. The frequency of ES may be anywhere within the range of 1.14 Hz to 1.80 Hz. Thus, a STWD system may result in a detuned non-optimal damper system.

6. SM Coupled with Multi-frequency TSWDs (MTSWD) Subjected to Dynamic Excitations

The STSWD system may not be very effective during a seismic eventuality. The efficiency loss due to detuning with respect to excitation frequency and structural frequency has been addressed through multiple frequency TSWD (MTSWD) system.

A symmetrical MTSWD system is devised with central frequency of 1.48 Hz and sloshing mass of 3.885 kg (μ =0.71% with respect to SM_5). The acrylic box at TL-1 has been retained as $TSWD_{280x80}$. The acrylic boxes at location TL-2 and TL-3 have been converted into combination of 85 mm wide $TSWD_{185x40}$ tuned with SM4 and 56 mm wide $TSWD_{265x40}$ tuned with SM_6 by fixing 4 mm thick acrylic sheet at suitable locations, as shown in Figure 18. Maximum sloshing mass (2.098 kg i.e. 54%) has been allocated to the central frequency of 1.48 Hz and 23% mass has been allocated to the frequencies 1.2Hz and 1.76Hz each.

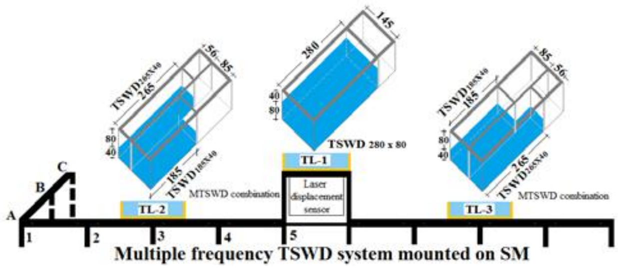

Fig. 18 Acrylic boxes converted as MTSWD System

This MTSWD system has been subjected different types of dynamic excitations in coupling with SM_4, SM_5 and SM_6. Its effectiveness with respect to bare SM displacement has been evaluated in Table 21.

Table 21: Performance of MTSWD systems coupled with SMs

Test Setup	Excitation Definition		Max. Displacement				Effectiveness Ratio *E* (%)	Specific Mass Ratio μ_s (%)
	Identification	A_{be}	Bare SM 'D_o'		SM-TSWD 'D_r'			
			Test Id	D_o (mm)	Test Id	D_r (mm)		
SM_4-MTSWD coupling; Mass ratio μ=0.93%;	Harmonic 1.76 Hz	0.75 mm	20/iii	12.66	79/ii	10.38	18.01	0.052
	El Centro (N-S)	0.064g	65-b	16.84	80/ii	14.4	14.49	0.064
	El Centro (E-W)	0.07g	66-b	15.89	81/ii	13.67	13.97	0.067
	BIS:1893 comp.	0.1g	67-b	14.64	82/ii	12.99	11.27	0.083
SM_5-MTSWD coupling; Mass ratio μ=0.71%;	Harmonic 1.48 Hz	0.75 mm	21/iii	12.24	87/ii	9.86	19.44	0.037
	El Centro (N-S)	0.064g	68-b	14.65	88/ii	13	11.26	0.063
	El Centro (E-W)	0.07g	69-b	16.23	89/ii	14.54	10.41	0.068
	BIS:1893 comp.	0.075g	70-b	14.55	90/ii	12.65	13.06	0.054
SM_6-MTSWD coupling; Mass ratio μ=0.63%;	Harmonic 1.2 Hz	0.75 mm	22/iii	12.06	95/ii	10.39	13.85	0.045
	El Centro (N-S)	0.04g	71-b	14.92	96/ii	13.44	9.92	0.064
	El Centro (E-W)	0.044g	72-b	16.08	97/ii	13.77	14.37	0.044
	BIS:1893 comp.	0.06g	73-b	13.39	98/ii	11.96	10.68	0.059

7. Performance Comparison of STSWD and MTSWD Systems

The observations recorded in table 20 and 21 are for STSWD and MTSWD systems respectively of equivalent mass ratios against identical dynamic excitations. The performance comparison of both the systems can be visualized by mass ratio required for 25% response reduction as given in Table 22.

Table 22: Performance Comparisons of STSWD and MTSWD Systems Coupled with SMs

SM Id	Excitation Designation	Mass Ratio for 25% Response Reduction (%)				Performance of MTSWD with Respect to STSWD Increase / (-) Decrease (%)
		STSWD		MTSWD		
		Specific Mass Ratio μ_s	Req. Mass Ratio μ	Specific Mass Ratio μ_s	Req. Mass Ratio μ	
SM_4	Harmonic 1.76 Hz	0.049	1.225	0.052	1.3	-6.12
	El Centro (N-S)	0.108	2.7	0.064	1.6	40.74
	El Centro (E-W)	0.162	4.05	0.067	1.675	58.64
	BIS:1893 comp.	0.168	4.2	0.083	2.075	50.6
SM_5	Harmonic 1.48 Hz	0.024	0.6	0.037	0.925	-54.17
	El Centro (N-S)	0.072	1.8	0.063	1.575	12.5
	El Centro (E-W)	0.082	2.05	0.068	1.7	17.07
	BIS:1893 comp.	0.053	1.325	0.054	1.35	-1.89
SM_6	Harmonic 1.2 Hz	0.054	1.35	0.045	1.125	16.67%
	El Centro (N-S)	0.121	3.025	0.064	1.6	47.11%
	El Centro (E-W)	0.068	1.7	0.044	1.1	35.29%
	BIS:1893 comp.	0.099	2.475	0.059	1.475	40.40%

The STSWD system has been optimally designed for 1.48 Hz frequency, the performance of STSWD in coupling with SM_5 is at best under resonant harmonic excitation of 1.48 Hz. However, against El Centro ground motion the effectiveness of MTSWD system, in coupling with SM_5 is better than the optimally tuned STSWD system. The performances of both the systems are similar against BIS:1893 compatible time history.

The effectiveness of MTSWD system in coupling with SM_4 and SM_6 is much better than the 23% detuned STSWD system under broad band earthquake excitations. It is observed that, for an ES in the assessed frequency range of 1.14 Hz to 1.8 Hz, specific mass ratio for STSWD system varies from 0.024 to 0.168. For the same ES, the specific mass ratio of MTSWD system varies from 0.037 to 0.083, exhibiting its robustness.

The maximum specific mass ratio of optimal STSWD system against broad band excitation is 0.0168 requiring a mass ratio of 4.2% for 25% effectiveness. The maximum specific mass ratio of MTSWD system, against all types of excitations considered, is 0.083 requiring a mass ratio of 2.08% for 25% effectiveness.

The effectiveness ratio of SM-MTSWD coupling is less than the optimal SM-STSWD coupling against well-defined harmonic excitations but the effectiveness of MTSWD system is spread over a range of structural and excitation frequency. For random and unpredictable dynamic excitations MTSWD system is more efficient and robust as compared to optimal STSWD system.

The displacement profiles of SMs in coupling with STSWD system and MTSWD systems, subjected to broad band excitations have been compared with respect to bare SM displacements in Figures 19, 20 and 21.

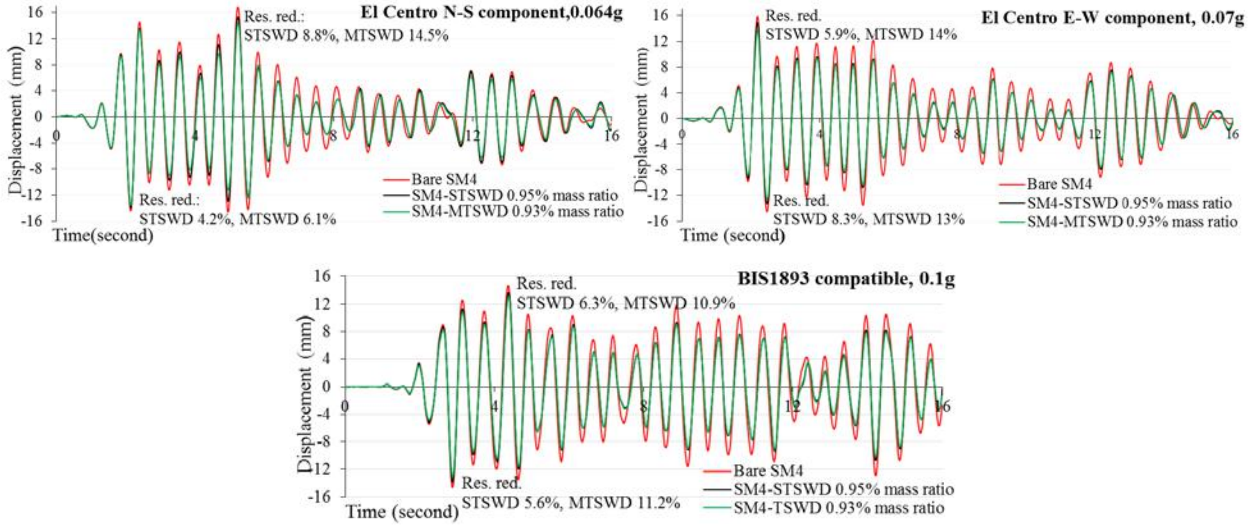

Fig. 19 Performance of comparison STSWD and MTSWD system coupled with SM4 subjected to broad band excitations

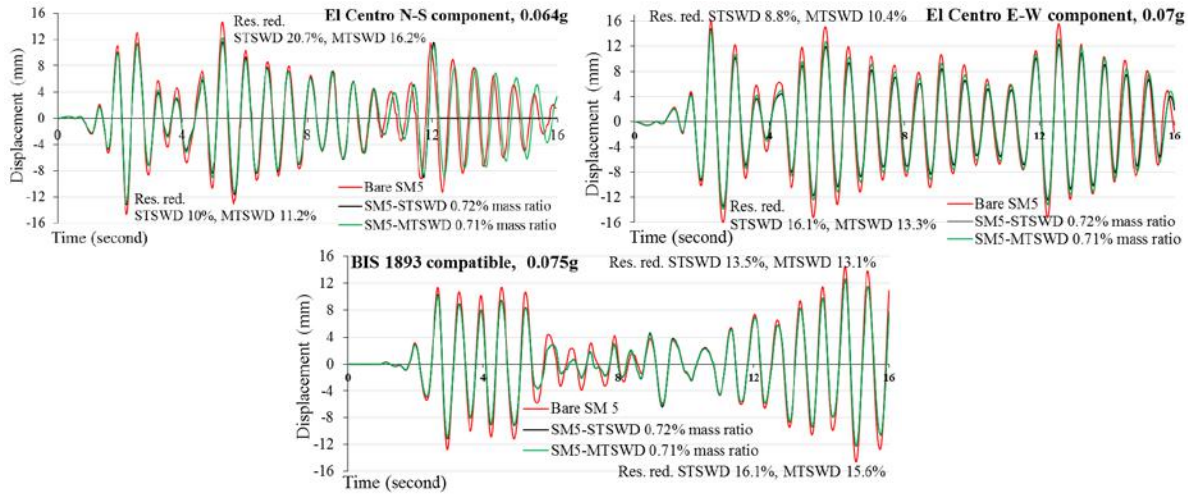

Fig. 20 Performance comparison of STSWD and MTSWD system coupled with SM5 subjected to broad band excitation

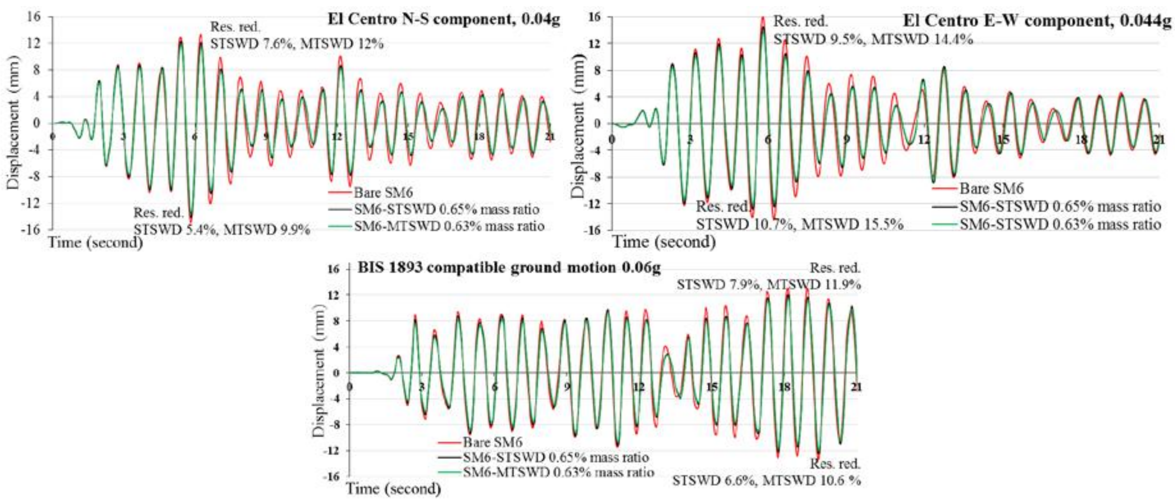

Fig. 21 Performance of STSWD and MTSWD system coupled with SM6 subjected to broad band excitation

CONCLUDING REMARKS

This study focuses on reducing the displacement response of non-seismically designed existing structures during seismic eventuality through a TSWD based response reducing regime. The proposal has been substantiated through a series of simulated shake table experiments on scaled models of an ES. The simulation has been derived by maintaining the dynamic properties of the ES, characteristics of the dynamic excitation, displacement of ES due to excitation and characteristics of the TSWDs as invariant between real life and laboratory environment.

The coupled behaviour of the ES and TSWD, for a robust response control performance, against different types of dynamic excitations, has been investigated. An empirical relation between effective damping ratio 'ξ_e' and mass ratio 'μ' has been derived as Equation (9), which is valid for wide range of frequencies (1.14 Hz to 1.8 Hz) to cover most of the existing medium height existing structures, designed with working stress philosophy, showing no sign of distress (damping ratio ≈ 3%).

For well-defined harmonic excitations, STSWD system is more suitable. The MTSWD provides a robust and efficient response reducing system for negotiating broad band excitations of approximately assessed existing structures. The present MTSWD combination of 56% sloshing mass allocation to central frequency and 23% to fringe frequencies should be further optimised through experimental investigations.

The performance of the MTSWD is tested, for the retrofitting effect on a reduced scale model having dynamic similitude with ES, for harmonic and broad band excitations. The experimental observations on SM are valid for ES. The ES can be retrofitted for 25 % response reduction against broad band excitation by providing TSWDs as given in Table 23.

Table 23: TSWDs on Real Life ES for 25% Response Reduction

Total Sloshing Mass Required (kg)	Alternative-1 with 80 mm Deep TSWDs				Alternative-2 with 160 mm Deep TSWDs			
	TSWD Id	Sloshing Mass (kg)	Number of TSWDs		TSWD Id	Sloshing Mass (kg)	Number of TSWDs	
			Required	Proposed			Required	Proposed
4234	$TSWD_{230x235}$	2.56	1654	1660	$TSWD_{275x280}$	5.26	805	820
9940	$TSWD_{285x280}$	4.13	2407	2420	$TSWD_{350x350}$	9.88	1007	1020
4234	$TSWD_{335x335}$	7.62	556	560	$TSWD_{490x455}$	21.7	196	200

The TSWDs of shallow depth are more efficient with respect quantitative use of water; however, from construction material considerations larger depth TSWDs may be more economical. These TSWDs can be accommodated on the roof of the ES in multi-layered clusters (Rai et al., 2013; Tamura et al., 1995).

The ES considered is representative of existing building stock. Requalification of most of the medium height existing structures designed and constructed with working stress principles to safety with all-time preparedness against seismic hazards is possible with TSWD based response reducing system. It addresses advantageously the serviceability, safety, and durability concerns as compared to other retrofitting measures. The economic parameters of the TSWD based retrofitting system may be further improved by integrating it with the plumbing system of ES to serve during the water distress and emergency water demand situations. The method is reliable, easy to execute, requires minimum post-execution maintenance, environmentally sustainable and cost effective.

REFERENCES

1. BIS: 456 (2000). "IS 456, Plain and Reinforced Concrete - Code of Practice (Fourth Revision)", Bureau of Indian Standards, New Delhi.
2. BIS: 1893 (2002). "IS 1893 (Part 1), Criteria for Earthquake Resistant Design of Structures: Part 1 General Provisions and Buildings (Fifth Revision)", Bureau of Indian Standards, New Delhi.

3. Bracci, J.M., Kunnath, S.K. and Reihnorn, A.M. (1997). “Seismic Performance and Retrofit Evaluation of Reinforced Concrete Structures”, ASCE Journal of Structural Engineering, Vol. 123, No. 1, pp. 3-10.
4. Chopra, A.K. (1995). “Dynamics of Structures: Theory and Applications to Earthquake Engineering”, Prentice Hall, USA.
5. Dolšek, M. and Fajfar, P. (2008). “The Effect of Masonry Infills on the Seismic Response of a Four-Storey Reinforced Concrete Frame-a Deterministic Assessment”, Engineering Structures, Vol. 30, No. 7, pp. 1991-2001.
6. Heidi Faison, Craig D. Comartin and Kenneth Elwood, (2004). “Housing Report, Reinforced Concrete Moment Frame Building without Seismic Details”, World Housing Encyclopaedia, an Encyclopaedia of Housing Construction in Seismically Active Areas of the World, EERI and IAEE, USA.
7. Holmes, M. (1961). “Steel Frames with Brickwork and Concrete Infilling”, Proceedings of the Institution of Civil Engineers, Vol. 19, pp. 473-478.
8. Ibrahim, R.A. (2005). “Liquid Sloshing Dynamics”, Cambridge University Press, New York, 2005.
9. Jain, S.K. and Jaiswal, O.R. (2007). “IITK-GSDMA Guidelines for Seismic Design of Liquid Storage Tanks”, Indian Institute of Technology, Kanpur.
10. Jaiswal, K.S., Sinha, R. and Goyal, A. (2002). “Reinforced Concrete Frame Building with Masonry Infill Walls Designed for Gravity Loads”, World Housing Encyclopaedia, an Encyclopaedia of Housing Construction in Seismically Active Areas of the World, EERI and IAEE, USA.
11. Koh, C.G., Mahatma, S. and Wang, C.M. (1995). “Reduction of Structural Vibrations by Multiple-mode Liquid Dampers”, Engineering Structures, Vol. 17, No. 2, pp. 122-128.
12. Kose, M.M. (2009). “Parameters Affecting the Fundamental Period of RC Buildings with Infill Walls”, Engineering Structures, Vol. 31, No 1, pp. 93-102.
13. Levy, S. and Wilkinson, J.P.D. (1976). “Generation of Artificial Time Histories Rich in all Frequencies from Given Response Spectra”, Nuclear Engineering Design, Vol. 38, pp. 241-251.
14. Li, H. and Wang Y. (2004). “Theoretical and Experimental Studies on Reduction for Multi-modal Seismic Response of High-rise Structure by Tuned Liquid Dampers”, Journal of Vibration and Control, Vol. 10, pp. 1041.
15. Manos, G.C., Triamataki, M. and Yasin, B. (1995). “Experimental and Numerical Simulation of the Influence of Masonry Infills on the Seismic Response of Reinforced Concrete Framed Structures”, Proceedings of the 10^{th} European Conference on Earthquake Engineering, Rotterdam, Vol. 3, pp. 1513-1518.
16. Marhatta, Y.B., Bothara, J.K., Magar, M.B. and Chapagain G. (2007). “Pillar Walaghar (URM Infilled RC Frame Buildings)”, World Housing Encyclopaedia, an Encyclopaedia of Housing Construction in Seismically Active Areas of the World, EERI and IAEE, USA.
17. Mehrabi, A.B., Shing, P.B., Schuller, M.P. and Noland, J.L. (1996). “Experimental Evaluation of Masonry Infilled RC Frames”, ASCE Journal of Structural Engineering, Vol. 122, No. 3, pp. 228-237.
18. Mondal, G. (2003). “Lateral Stiffness of Unreinforced Brick Infilled RC Frame with Central Opening”, Master of Technology Thesis, Department of Civil Engg., Indian Institute of Technology Kanpur, India.
19. Mukherjee, S. and Gupta, V.K. (2002). “Wavelet Based Generation of Spectrum-compatible Time Histories”, Soil Dynamics and Earthquake Engineering, Vol. 22, pp. 799-804.
20. Nawrotzki P. (2005). “Visco-elastic Devices for the Seismic Control of Machinery Equipment and Buildings”, Pro. of 9^{th} World Seminar on Seismic Isolation, Energy Dissipation and Active Vibration Control of Structures, Kobe, Japan.
21. Newmark, N.M. and Hall, W.J. (1978). “Development of Criteria for Seismic Review of Nuclear Power Plants”, NUREG/CR-0098, U.S. Nuclear Regulatory Commission, Washington D.C.
22. Park, J. and Reed, D. (2001). “Analysis of Uniformly and Linearly Distributed Mass Dampers under Harmonic and Earthquake Excitation”, Engineering Structures, Vol. 23, pp. 802-814.

23. Pires, F., Campos-Costa, A. and Raposo, S. (1995). "Hysteretic Behaviour of R/C Frames Infilled with Brick Masonry Walls", Proceedings of the 10th European Conference on Earthquake Engineering, A.A. Balkema, Rotterdam, Vol. 3, pp. 1739-1744.
24. Rai, N.K., Reddy, G.R. and Venkatraj, V. (2011). "Effectiveness of Multiple TSWDs for Seismic Response Control of Masonry In-filled RC Framed Structures", ISET Journal of Earthquake Technology, Vol. 48 No. 2-4, pp. 85-101.
25. Rai, N.K., Reddy, G.R., Venkatraj, V. and Dubey, P.N. (2013). "Seismic Retrofitting of Existing Structures by Tuned Sloshing Water Damper: An Experimental Study", ISET Journal of Earthquake Technology, Vol. 50, No. 1, pp. 27–47.
26. Rodrigues, H., Varum, H. and Costa, A. (2010). "Simplified Macro-model for Infill Masonry Panels", Journal of Earthquake Engineering, Vol. 14, No. 3, pp. 390-416.
27. Sabnis, G.M., Harris, H.G., White, R.N. and Mirza, M.S. (1983). "Structural Modelling and Experimental Techniques", Prentice Hall Inc., Engelwood Cliff, New Jersey.
28. Shedid, M. (2006). "Ductility of Reinforced Concrete Masonry Shear Walls", M. A. Sc. Thesis, Department of Civil Engineering, McMaster University, Ontario, Canada.
29. Sharma, A., Reddy, G.R. and Vaze, K.K. (2012). "Shake Table Tests on a Non-seismically Detailed RC Frame Structure", Structural Engineering and Mechanics, Vol. 41, No. 1, pp. 1-24.
30. Tait, M.J. (2008). "Modelling and Preliminary Design of a Structure-TLD System", Engineering Structures, Vol. 30, pp. 2644–2655.
31. Tamura, Y., Fujii, K., Ohtuski, T., Wakahara, T. and Kohsaka, R. (1995). "Effectiveness of Tuned Liquid Dampers under Wind Excitation", Engineering Structures, Vol. 17, No. 9, pp. 609-621.
32. Valiasis, T.N. and Stylianidis, K.C. (1989). "Masonry Infilled R/C Frames under Horizontal Loading –Experimental Results", European Earthquake Engineering, Vol. 3, No. 3, pp. 10-20.
33. Yalla, S.K. (2001). "Liquid Dampers for Mitigation of Structural Response: Theoretical Development and Experimental Validation", Ph.D. dissertation, Dept. of Civil Engineering and Geological Sciences, Notre Dame, Indiana, USA.
34. Yu, Jin-Kyu, (1999). "Nonlinear Characteristics of Tuned Liquid Dampers", Ph.D. Thesis, University of Washington, United States.